Hindawi
Journal of Combustion
Volume 2018, Article ID 8406754, 27 pages
https://doi.org/10.1155/2018/8406754

Review Article

Review of Oxidation of Gasoline Surrogates and Its Components

J. A. Piehl,[1] A. Zyada,[1] L. Bravo,[2] and O. Samimi-Abianeh[1]

[1]*Mechanical Engineering Department of Wayne State University, Detroit, MI 48202, USA*
[2]*Propulsion Division, Vehicle Technology Directorate, MD, USA*

Correspondence should be addressed to O. Samimi-Abianeh; o.samimi@wayne.edu

Received 14 July 2018; Revised 5 November 2018; Accepted 13 November 2018; Published 6 December 2018

Academic Editor: Constantine D. Rakopoulos

There has been considerable progress in the area of fuel surrogate development to emulate gasoline fuels' oxidation properties. The current paper aims to review the relevant hydrocarbon group components used for the formulation of gasoline surrogates, review specific gasoline surrogates reported in the literature, outlining their utility and deficiencies, and identify the future research needs in the area of gasoline surrogates and kinetics model.

1. Introduction

Surrogate fuels, comprising a small number of components, are formulated to simulate complex real fuels. Design of surrogate mixtures is usually focused on the emulation of a particular property of the target fuel such as evaporation, e.g., [1–4], thermodynamic properties, e.g., [5–9], or combustion characteristics, e.g., [10–13]. Some advanced surrogates were also proposed to mimic a majority of the fuel properties simultaneously, e.g., [14–20].

Gasoline is the major transportation fuel in the United States and includes n-alkanes, iso-alkanes, naphthenes, olefins, aromatics, and oxygenated groups with different distributions depending on the season, market place, crude source, and refinery processes. An example of the chemical composition of gasoline can be seen in Table 1. United States and European gasoline may contain naphthenes up to 16% and 9 % by volume, respectively, which may be converted to aromatics in the refinery process [21, 22]. It is a good practice to include a component from the major hydrocarbon group in fuel blend surrogates for emulating ignition delay, laminar flame speed, and fuel speciation. However, it is a challenge to generate predictive kinetic mechanisms for each individual surrogate component or hydrocarbon group while maintaining suitable mechanism size for computational fluid dynamics (CFD) applications. The physical properties of several components relevant to gasoline fuel and its surrogates are presented in Table 2.

In this review and research paper, the hydrocarbon groups and components relevant to gasoline fuel and eleven surrogate mixtures reported in the literature are reviewed and modeled. Modeling predictions for the evaporation and autoignition, produced as part of this work, are compared with measured gasoline data at available conditions in the literature. The main objective of the paper is to study advanced gasoline surrogates relevant to Homogenous Charge Compression Ignition (HCCI) engines. Therefore, only autoignition will be explored in this work. The experiments and chemical kinetic models for hydrocarbon groups and pure components relevant to gasoline fuel are studied and discussed in the following section.

2. Chemical Kinetic Models and Properties of Gasoline Hydrocarbon Groups

In this section six major gasoline hydrocarbon groups (n-alkane, iso-alkane, olefin, cycloalkane, aromatics, and oxygenated groups) and the relevant components to gasoline fuel are reviewed and discussed.

2.1. N-Alkane Group. Gasoline is a complex fuel consisting of many components including a variety of hydrocarbons ranging from C_3 to C_{12+} as shown in Table 1. One of the major component groups in gasoline is n-alkane, which constitutes approximately 9.5% of the fuel as shown in Table 1. Some

Table 1: Gasoline Research and Development (RD387) mixture composition by using gas chromatography (GC). Data are in volume fraction. "0.000" entry means the component concentration of less than 10 ppm [Internally measured for a sample of RD387].

C#	n-alkane	iso-alkane	olefin	naphthene	aromatic	not classified	total per carbon
C_3	0.112	0.000	0.000	0.000	0.000	0.000	0.112
C_4	2.201	0.306	0.009	0.000	0.000	0.000	2.516
C_5	1.023	4.332	1.527	12.253	0.000	0.000	19.135
C_6	0.697	9.873	2.380	0.830	0.588	0.000	14.368
C_7	4.361	13.183	0.542	1.789	10.489	0.000	30.362
C_8	0.634	11.320	0.270	0.828	7.381	0.000	20.432
C_9	0.248	2.427	0.006	0.224	4.738	0.185	7.826
C_{10}	0.085	0.682	0.000	0.044	2.359	0.230	3.399
C_{11}	0.061	0.092	0.000	0.000	0.773	0.168	1.095
C_{12+}	0.066	0.042	0.000	0.000	0.078	0.569	0.756
Total	9.487	42.257	4.733	15.966	26.405	1.153	100.0

Table 2: Some of the gasoline fuel component representatives.

	Group name	Boiling temp. (°C)	Density (kg/m^3)	RON/MON
n-butane	n-alkane	0	2.8	94/90.1
n-heptane	n-alkane	100	684	0/0
iso-octane	iso-alkane	99	690	100/100
2-methylbutane (iC_5H_{12})	iso-alkane	28	616	110/97
2-methylpentane (iC_6H_{14})	iso-alkane	61	650	92/90
2-methylhexane	iso-alkane	90	670	42/46
toluene	aromatics	110	867	118/103
ethanol	oxygenate	78	789	108/90
1-pentene	olefin	30	641	90.9/77.1
trans-2-pentene	olefin	30	649	94/80
trans-2-hexene	olefin	63	669	73.4/68.6

of the properties of the alkanes up to C_{12} are shown in Table 3, with n-butane holding the lowest boiling temperature of -1°C and n-heptane having a boiling temperature of 98°C. In Figure 1, the ignition delay times of several n-alkanes are simulated and compared with gasoline measured data. From this model, some general trends can be observed, such as a decrease in the ignition delay time by increasing the carbon chain length. Another significant note is that the ignition delay times of n-nonane, n-decane, n-undecane, and n-dodecane are almost identical, despite the increasing length of the carbon chain.

There has been increasing research in the low-temperature combustion regime as more engine manufacturers have been seeking this operating condition to improve fuel efficiency and decrease harmful emissions, e.g., [35]. N-alkanes, especially larger n-alkanes, are known to be reactive during low-temperature combustion [36]. Since n-alkanes are used to mimic the combustion characteristics of gasoline fuel; e.g., [19], it is crucial to understand if the surrogate models will accurately model the fuel during low-temperature oxidation. The chain length of the n-alkane has a tremendous effect on the cool flame reactivity and current gasoline surrogate models have poor results when it comes to modeling oxidation behavior in these regions, e.g., [35].

N-heptane has been historically used as a representative of the n-alkane group due to its octane number and its concentration in gasoline fuel (4.3% by volume), as shown in Table 1. The n-heptane kinetic model has been developed, reevaluated, and validated many times, e.g., [13, 37–39].

Another major component in gasoline is n-butane, as shown in Table 1. Combustion kinetics of n-butane has been well determined, and Simmie [40] reviewed the n-butane model developments and experiments. N-butane has a boiling temperature of 23.7°C and might be one of the main reasons that gasoline has a low boiling temperature.

Westbrook et al. [41] developed a detailed chemical kinetic model to describe the pyrolysis and oxidation of nine n-alkanes, from n-octane to n-hexadecane. The model allows the simulation of both low and high temperature chemistry of these n-alkanes and has been evaluated extensively by data from shock tubes, flow reactors, and jet-stirred reactors.

In a recent study, Cai et al. [42] have optimized the rate rules for n-alkanes for further kinetic model optimization. Cai et al. [42] model is based on the model created by Sarathy et al. [43] for the oxidation of n-alkanes from C_8 to C_{16} and

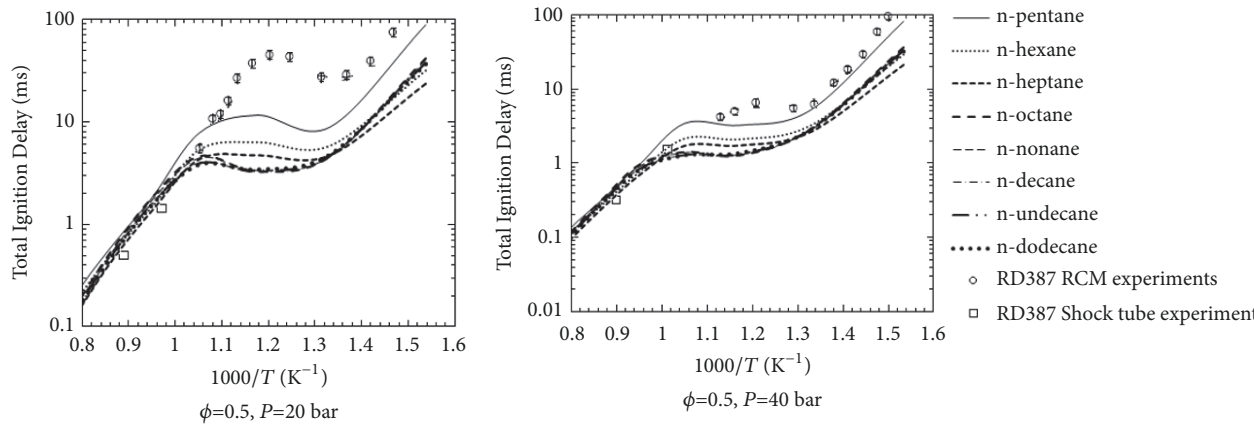

Figure 1: Simulated ignition delay times for the pure components in air at a pressure of 20 and 40 bar and equivalence ratio of Φ=0.5. Simulations were carried out using Samimi Abianeh et al. [19] kinetic model in an adiabatic constant-volume model. Gasoline RD387 ignition delay experimental data were taken from Kukkadapu et al. [23] and Gauthier et al. [10] for comparison purpose.

Table 3: n-Alkane group component properties.

	Liquid density (kg/m^3)	Boiling point (°C)	RON/MON (-/-)	Lower heating value (MJ/kg)
n-butane	583	-1	94/89.1	45.84
n-pentane	626	36	62/63.2	45.34
n-hexane	654	69	25/26	45.10
n-heptane	683	98	0/0	44.56
n-octane	703	126	-10/-10	44.86
n-nonane	718	151	-10/-10	44.62
n-decane	730	174	-15/-15	44.56
n-undecane	740	196	-15/-15	44.52
n-dodecane	750	216	-20/-20	44.23

Bugler et al. [44] model for low-temperature kinetics. The chemical mechanism was automatically generated using a Bayesian approach for the n-alkane model and was compared to experimental data. The model showed improved results for a variety of alkanes compared to the previous models.

2.2. Iso-Alkane Group. Iso-alkanes are the largest of the major hydrocarbon groups found in gasoline as shown in Table 1. 42.3 % by volume of the research grade gasoline, RD387, is composed of iso-alkane components as shown in Table 1. Historically, 2,2,4-trimethylpentane (also known as iso-octane) has been utilized as the surrogate for the iso-alkane group since the surrogate mixture of 2,2,4-trimethylpentane and n-heptane mimics gasoline combustion to a good degree of accuracy. Both fuels could be produced in significant amount and have very similar density, hydrogen to carbon (H/C) ratio, and lower heating value. Gasoline includes about 11% of iso-octane as shown in Table 1. Octane has 18 isomers and only 2,2,4-trimethylpentane and n-octane have been studied extensively and the detailed mechanism and validation for n-octane can be found in [43, 45] and iso-octane in [25, 46, 47]. As reviewed by Simmie [40], the n-octane model of Glaude et al. [45] and other available models have required improvement for the secondary reactions of alkenes which are the main primary products during the oxidation of n-octane. Atef et al. [48] recently created a new kinetic model for 2,2,4-trimethylpentane with improved reaction rates, group values, and rate rules. In addition, an alternative pathway for the isomerization of peroxy-alkyl hydroperoxide and other O_2 addition reactions were added. These additional reactions improved the predictions for the reactions at lower equivalence ratios, around 0.25. Furthermore, the updated model highlighted the need for further reaction pathways at lower temperatures, as the 3rd O_2 reaction pathways showed significant changes to the lower temperature combustion.

Isomers of C_7 components in the iso-alkane group have a higher volume fraction than isomers of C_8 components as shown in Table 1. C_7 has 9 isomers, including n-heptane, as shown in Table 4 and Figure 2. Isomers of C_7 have barely been studied. Westbrook et al. [24] developed a high temperature detailed mechanism for all nine isomers of heptane but due to lack of experimental data only n-heptane was validated. Westbrook et al. [49] later improved the mechanism by adding a new reaction group to the previous mechanism, in which hydroperoxyalkyl radicals that originated from the abstraction of an H atom from a tertiary site in the parent heptane molecule are assigned to new reaction sequences involving additional internal H atom abstractions. Also, the rates of hydroperoxyalkylperoxy radical isomerization reactions have all been reduced so that they are equal to rates

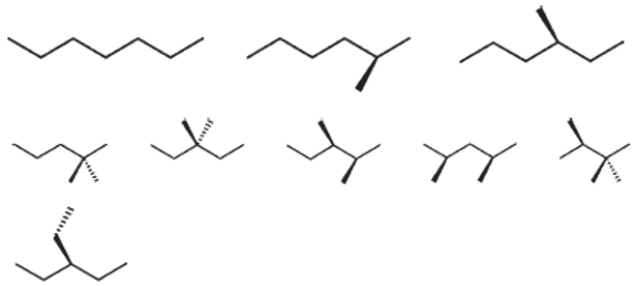

Figure 2: Heptane isomers Top: most reactive, Middle: least reactive, and Bottom: intermediate reactivity. Picture is adopted from [24].

Table 4: Properties of isomers of heptane, adapted from [24].

Chemical name	Short name	RON	MON	Cetane number
n-Heptane	nC_7H_{16}	0	0	56
2-Methyl hexane	$2C_7H_{16}$	42	46	38
3-Methyl hexane	$3C_7H_{16}$	52	56	33
2,2-Dimethyl pentane	$22C_7H_{16}$	93	96	13
3,3-Dimethyl pentane	$33C_7H_{16}$	81	87	19
2,4-Dimethyl pentane	$24C_7H_{16}$	83	84	18
2,3-Dimethyl pentane	$23C_7H_{16}$	91	89	14
3-Ethyl pentane	$3C_7H_{16}$	65	69	27
2,2,3-Trimethyl butane	$223C_7H_{16}$	112	112	4

Table 5: Experimentally and numerically predicted values for critical compression ratios of hexane isomers [51].

	Experimental/Computational critical compression ratio	RON
n-hexane	6.4/5.7	25
2-methyl pentane	8.1/8.75	73
3-methyl pentane	8.4/8.75	75
2,2-dimethyl butane	11.5/10.5	92
2,3-dimethyl butane	19.0/14.5	104

of analogous alkylperoxy radical isomerizations to improve the agreement between computed and available experimental ignition delay times in rapid compression machines (RCMs). Computed results fall into three general groups as shown in Figure 2: the most reactive isomers, including n-heptane, 2-methyl hexane, and 3-methyl hexane; the least reactive isomers, including 2,2-dimethyl pentane, 3,3-dimethyl pentane, 2,3-dimethyl pentane, 2,4-dimethyl pentane, and 2,2,3-trimethyl butane; and the remaining isomer with an intermediate level of reactivity, 3-ethyl pentane. These observations are approximately consistent with the octane rating of each isomer in Table 4. Recently, 2-methyl hexane has been studied by Mohamed et al. [50]. The focus of their study was on updating thermodynamic data and the kinetic reaction mechanism for 2-methyl hexane based on recently published thermodynamic group values and rate rules derived from quantum calculations and experiments.

Table 6: Pentane isomers' properties and autoignition criteria for stoichiometric hydrocarbon/air mixtures, adopted from [52].

	Isopentane		Neopentane		nPentane	
RON	92.3		85.5		61.7	
p (torr)	300	400	300	400	300	400
T (K)	700	690	670	665	650	650
	NTC zone		NTC zone		NTC zone	
T_{min} (K)	730	730	770	775	755	755
T_{max} (K)	820	820	880	860	850	845
	CF zone		CF zone		CF zone	
T_{min} (K)	700	700	685	665	670	665
T_{max} (K)	755	755	880	890	840	845

Isomers of hexane are the third major group in gasoline after isomers of heptane and octane. Hexane has five isomers as shown in Table 5. Curran et al. [51] developed a kinetic model for all the isomers of hexane and utilized the model in a 3D CFD program to study autoignition during engine combustion to develop the kinetic model. The compression ratio of the engine was continuously increased to reach the critical compression ratio where hexane isomer autoignition is possible as reported in Table 5. The autoignition of three isomers of hexane is studied by using the detailed mechanism of [25] in the current work as shown in Figure 3. The difference between the computed ignition delay times of two isomers, 2-methyl pentane and 2,2-dimethyl butane, is insignificant. However, the difference between the critical compression ratios of the two isomers is 3.4, quite a big difference. This discrepancy could be due to deficiencies of the detailed mechanism of [25] to reproduce the ignition delay times of hexane isomers.

Isomers of pentane are the other major components in the hydrocarbon mixture of gasoline as shown in Table 1. Three isomers of pentane are n-pentane, iso-pentane (2-methylbutane), and neopentane (2,2, dimethylpropane). Ribaucour et al. [52] studied the isomers of pentane using a RCM to examine the influences of variations in the fuel molecular structure on the isomers' autoignition characteristics. They studied the pentane isomers autoignition at initial gas temperatures between 640 K and 900 K and a precompression pressure of 300 and 400 torr. The pentane isomers experienced a two-stage autoignition in most cases. At the highest compression temperature achieved, little or no first-stage ignition is observed. The first stage follows a low-temperature alkylperoxy radical isomerization pathway that is effectively quenched when the temperature reaches a level where dissociation reactions of alkylperoxy and hydroperoxyalkylperoxy radicals are more rapid than the reverse addition steps. The second stage is controlled by the onset of the dissociation of hydrogen peroxide. A summary of the Ribaucour et al. [52] RCM experiments is shown in Table 6. A detailed mechanism was also developed from the findings and validated against the RCM data in [52]. Bugler et al. [44] measured ignition delay times of n-pentane, iso-pentane, and neo-pentane mixtures in two shock tubes and in a RCM. This study presented ignition delay time data for

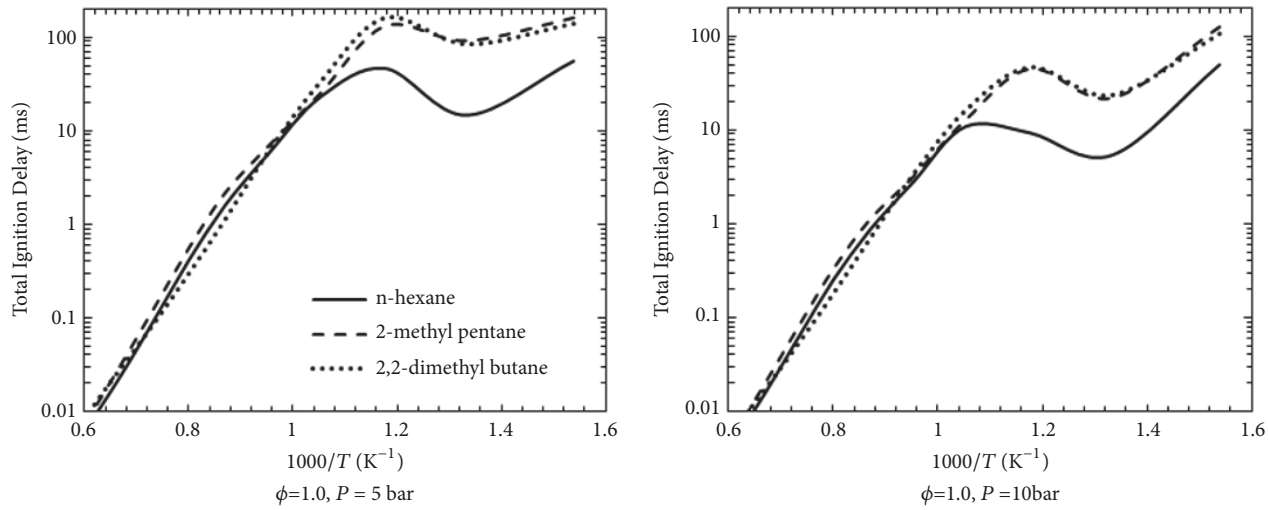

Figure 3: Simulated ignition delay times for the hexane isomers in air at pressures of 5 and 10 bar and an equivalence ratio of Φ=1. Simulations were carried out using the kinetic mechanisms as developed by [25] in an adiabatic constant-volume model.

the pentane isomers at equivalence ratios of 0.5, 1.0, and 2.0 in air at pressures of 1, 10, and 20 atm in the shock tube, and 10 and 20 atm in the RCM, as well as data at an equivalence ratio of 1.0 in 99% argon, at pressures near 1 and 10 atm in the shock tube. A detailed chemical kinetic model was also used to simulate the experimental ignition delay times, and these are well-predicted for all of the isomers. Kang et al. [53] studied the autoignition characteristics of the three C_5 isomers, n-pentane, 2-methylbutane (iso-pentane), and 2,2-dimethylpropane (neo-pentane) using a CFR engine. Stronger two-stage heat release for n-pentane with respect to neo-pentane was observed. In contrast, single-stage heat release was observed for iso-pentane, leading to the weakest overall oxidation reactivity of the three isomers.

Nonane has 35 isomers (including n-nonane) and they are one of the major components of iso-alkanes in the gasoline mixture by a volume fraction of 2.4% as shown in Table 1. However, none of the isomers of nonane, except 2-methyl-octane [43], were studied and developed at the time of writing.

2.3. Olefin Group. Olefins, also known as alkenes, compose a large amount of transportation fuels such as gasoline, diesel, and aviation fuel. For example, gasoline consists of 15-20% olefins by volume [54]. Additionally, olefins have been identified as a crucial component in determining the octane sensitivity of the fuel, an important trait for spark-ignition engines. Furthermore, the oxidation of the alkenes is an important submechanism in the combustion of higher alkanes. The majority of olefins in gasoline are C_5 and C_6 components as shown in Table 1. Mechanism models and ignition delay experiments of some of the C_5 and C_6 components were studied and discussed in [13, 40, 54–56].

Pentene has six isomers: 1-pentene (RON = 90.9 and MON = 77.1 [57]), cis-2-pentene (unknown octane number), trans-2-pentene (RON = 94 and MON = 80 [57]), 2-methyl-1-butene (RON = 100.2 and MON = 81.9 [API]),

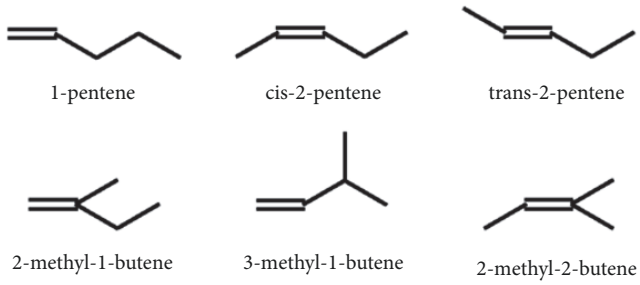

Figure 4: Pentene isomers.

2-methyl-2-butene (RON = 97.3 and MON = 84.7 [58]), and 3-methyl-1-butene (unknown octane number) as shown in Figure 4. Mehl et al. [56] studied low-temperature branching mechanisms for alkenes and developed a kinetic model for n-hexene (1-hexene, trans-2-hexene, and trans-3-hexene) isomers. In a different study, Mehl et al. [13] studied two isomers of pentene (1-pentene and trans-2-pentene) and three isomers of hexene (1-hexene, trans-2-hexene, and trans-3-hexene) using a shock tube and developed a kinetic model for them. The ignition delay times of some of the isomers of pentene and hexene are shown in Figure 5 by using the model of Mehl et al. [13]. Westbrook et al. [54] studied the autoignition of 2-methyl-2-butene by using a shock tube and jet-stirred reactor (JSR) and developed a corresponding kinetic model. The shock tube experiments were carried out at three different pressures (approximately 1.7 atm, 11.2 atm, and 31 atm), at three different equivalence ratios (0.5, 1.0, and 2.0) and experienced initial postshock temperatures between 1330K and 1730K. The JSR experiments were performed at nearly atmospheric pressure (800 torr), stoichiometric fuel/oxygen mixtures with a 0.01 mole fraction of 2-methyl-2-butene fuel, and a residence time in the reactor of 1.5s. The mole fractions of 36 different chemical species were measured over a temperature range from 600 K to 1150 K in this experiment.

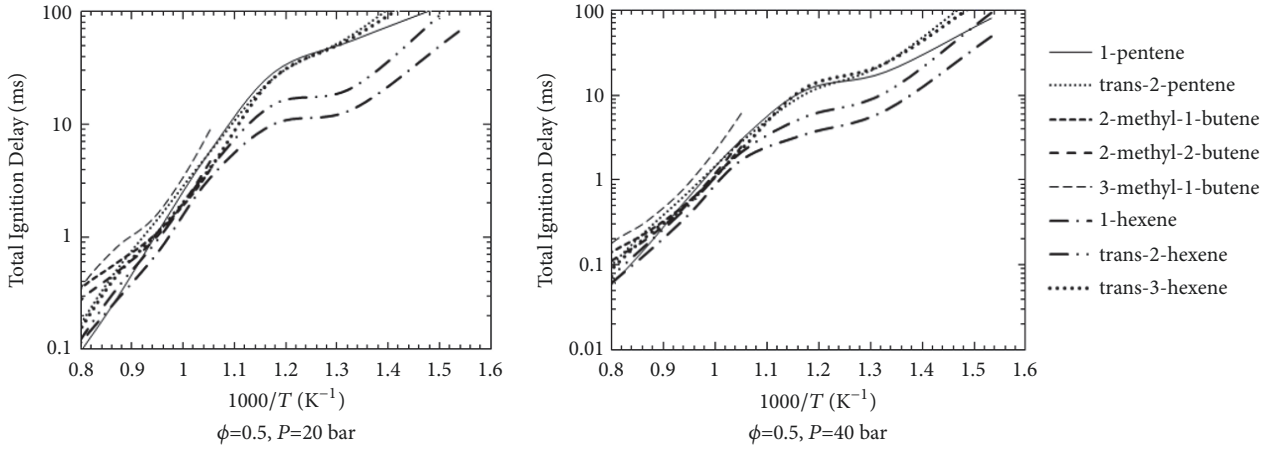

Figure 5: Simulated ignition delay times for the pentene and hexene isomers in air at pressures of 20 and 40 bar and an equivalence ratio of 0.5. Simulations were carried out using Mehl et al.'s [13] model in an adiabatic constant-volume model.

Westbrook et al. [54] concluded that at high temperatures this olefinic fuel reacts rapidly, similar to related alkane fuels, but the pronounced thermal stability of the allylic pentenyl species inhibits low-temperature reactivity; so 2-methyl-2-butene does not produce cool flames or negative temperature coefficient (NTC) behavior as shown in Figure 5. The lack of NTC behavior is related to the high octane sensitivity of 2-methyl-2-butene, whereas the lack of low-temperature reactivity is due to the low reactivity of small allylic radical species at lower temperatures. This low-temperature stability is a result of the radicals' inability to produce alkenylperoxy radicals that could lead to NTC behavior. Generally, low-temperature oxidation of components was found to be fastest for n-alkane, followed by 1-alkene, 2-alkene, and then 3-alkene (if it exists in components such as 3-hexene) as shown in Figure 5 and explained by Leppard [59]. The NTC behavior decreases as the carbon-carbon double bond moved away from the end of the carbon chain and nearly disappears for 3-hexene [54]. Trans-2-pentene and trans-3-hexene show identical autoignition behaviors as shown in Figure 5. The pentene and hexene isomers have unique high temperature ignition delay times, juxtaposed to the previously studied components such as n-alkanes and iso-alkanes (e.g., compare Figures 1 and 3 with Figure 5). Westbrook et al. [54] found the pressure exponent of -0.4 for 2-methyl-2-pentene. These pressure exponents are smaller than the gasoline fuel pressure exponent (around -1.06) and make these isomers good fuel additive choices for limiting knock in highly boosted spark-ignition gasoline engine. Minetti et al. [60] studied the ignition delay and speciation of 1-pentane and 1-pentene using a RCM in a temperature range of 600-900 K and pressures of 7 to 8 bar. They found some similarities and major differences in the behavior of 1-pentane and 1-pentene. The similarities are due to the fact that 1-pentene is a primary product of the oxidation of n-pentane and the presence of intermediate unstable species (i.e., $RO_2{}^*$ and $^*QOOH$) belonging to both hydrocarbons. The major difference is due to effect of the carbon-carbon double bond in 1-pentene, allowing HO_2 and OH to add. 1-pentene also favors allylic hydrogen abstraction in the first attack and in the isomerization of intermediate radicals.

Hexene has seventeen isomers; of those seventeen, the most studied isomers are 1-hexene, trans-2-hexene, and trans-3-hexene, e.g., [55, 61, 62]. Wagnon et al. [55] studied three hexene isomers (1-hexene, trans-2-hexene, and trans-3-hexene) using a RCM. The measurements of stable intermediates showed significant differences in the isomer reaction pathways. Measurements of the three hexene fuels indicate the initial oxidation of the three isomers proceeds at similar rates. The length of the alkyl chain determines the reaction pathways and what stable intermediates are produced during the oxidation. Using the Mehl et al. [13] model, the model and the experimental data showed good agreement with the autoignition characteristics; however, there were some deviances for the expected amounts of propanal. The results for trans-3-hexene were especially troubling, as the model overpredicted the propanal production by a factor of ten. Additionally, the model overpredicted the consumption rate of hexene for all the isomers. The results from Wagnon et al. support the need to develop better reactionary models to more accurately predict the reactionary pathways and sensitivity of different molecular structures. Yahyaoui et al. [63–65] derived correlations to relate the ignition delay times of 1-hexene to changes of temperature and equivalence ratio by using shock tube data. Yang et al. [61, 62] derived the correlation for three hexene isomers (1-hexene, 2-hexene, and 3-hexene) to relate the ignition delay to pressure, temperature, and equivalence ratio using new measured data from a shock tube. Yang et al. discerned the pressure exponent of -0.53 for 1-hexene and 2-hexene and -0.421 for 3-hexene.

Leppard [59] studied the chemistry of the autoignition of alkenes (1-butene, cis-2-butene, iso-butene, 2-methyl-2-butene, and 1-hexene) and their corresponding alkanes (n-butane, iso-butane, 2-methylbutane, and n-hexane) using a motored, single-cylinder engine by measuring stable intermediate species. Leppard produced evidence that the chemistry of the autoignition of an alkene is dominated by radicals

adding to the double bond, especially for the lower carbon number compounds.

2.4. Cycloalkane Group. Cycloalkanes (also known as naphthenes) constitute a significant portion of conventional diesel, jet fuel, and gasoline (up to 35%, 20%, and 15% by volume, respectively). Methyl substituted (mono and di) cycloalkane isomers predominate in gasoline fuel, with more numerous methyl and alkyl substitutions less prevalent [21]. C_5 cycloalkanes are the most abundant components in gasoline as shown in Table 1. Limited studies, whether experimental or computational, have been performed on the oxidation of cycloalkanes, e.g., [66–74]. The kinetic mechanisms of cyclopentane and cyclohexane have been studied the most out of all the cycloalkanes due to their simplicity. The autoignition of cyclohexane has been studied using shock tubes [75–77], RCMs [26, 70, 78], JSRs [72, 74], plug-flow reactors [79, 80], and closed reactors [81–84]. The ignition characteristics of cyclopentane were studied using shock tubes [75, 76, 85] and a JSR [86]. The autoignition of cyclopentane and cyclohexane was observed to be more pressure dependent than olefins. This can be displayed in the study done by Daley et al. [75], where they discovered the pressure exponents of cyclopentane and cyclohexane at stoichiometric conditions are 0.9 and 1.1, respectively. Comparatively, the pressure exponents at the same conditions for 2-methyl-2-butene and 1-hexane are -0.4 and -0.3, respectively. The kinetic mechanisms of cyclopentane and cyclohexane need improvements as discussed by [75] due to their unreliability and inaccuracy. The cyclohexane kinetic model studied was developed by Silke et al. [26] and was compared to RCM ignition delay data of [70], as shown in Figure 6. The model predicts the ignition delay trends well, even in the NTC region. However, the overall ignition delay was overpredicted for most of the measured points. Further research was done on methyl substituted isomers of cycloheptane and cyclohexane. Pitz et al. [21] developed a methylcyclohexane model at low and high temperatures and attempted to validate it using RCM data. Again, the model overpredicted the ignition delay, especially at low temperatures.

2.5. Aromatic Group. Aromatics are another major component in gasoline, as shown in Table 1 and Figure 7. Benzene, a common aromatic, is limited to 1% of the total volume of gasoline sold in the United States [87]. The most abundant aromatics in gasoline sold in the US are toluene and m-xylene (1,3-dimethylbenzene) [21]. Toluene is added to US gasoline and it could be the reason behind the C_7 peak in Table 1. In addition to US gasoline, toluene is the major aromatic component in Chinese finished gasoline (RON=93), Japanese finished regular gasoline (RON=90), and Japanese finished premium gasoline (RON=100) as shown in Table 7. Three additional major aromatics are shown in Table 7: 1,2,4-trimethylbenzene, 1-methyl 3-ethylbenzene, and m-xylene.

Chemical kinetic models of toluene have been extensively studied. Some of the more recent studies are [13, 88–90] with autoignition experiments in [27, 88, 89, 91–93]. Toluene does not show low-temperature or NTC reactivity due to its high RON/MON of 126/110. Three kinetic models were used by [94] to model the ignition delay of toluene and were compared with experimental shock tube data as shown in Figure 8. As shown in the figure, the modeled ignition delay times are in fair agreement with the experimental data. As reported by [27], the ignition delay pressure dependence of -1.09 at an equivalence ratio of 1 is close to the ignition delay pressure exponent of gasoline of -1.06. An interesting thing to note is that the ignition delay of toluene is more sensitive to pressure changes than cycloalkane and olefin components.

1,2,4-trimethylbenzene (124TMB) is another major gasoline component in the aromatic group as shown in Table 7. Much like toluene, 124TMB does not show low-temperature reactivity due to its high RON/MON of 115/110. 124TMB is a popular surrogate for modeling kerosene [95], with a kinetic model that was studied and developed in [96, 97]. The combustion characteristics of 124TMB have been studied by a shock tube [98], RCM [31], JSR [99], burner stabilized premixed flames [100, 101], counter-flow burner [102], and freely propagating premixed flames [103]. Roubaud et al. [31] studied the autoignition of 11 alkylbenzenes in a RCM at stoichiometric conditions, with a temperature range of 600 K to 900 K and compressed pressures up to 25 bar. Their experiments showed toluene, m-xylene, p-xylene, and 1,3,5-trimethylbenzene ignite only at temperatures above 900 K and 16 bar, while o-xylene, ethylbenzene, 1,2,3-trimethylbenzene, 1,2,4-trimethylbenzene, n-propylbenzene, 2-ethyltoluene, and n-butylbenzene ignite at much lower temperatures and pressures. The ignition delay times for all 11 of these components are shown in Figure 9. Among these 11 components, 124TMB has the greatest ignition delay time which correlates to the lowest reactivity of all the components. Hui et al. [102] confirmed the low reactivity of 124TMB among other aromatic components (toluene, n-PB, and 1.3.5TMB) through their laminar flame speed study in a twin-flame counter-flow reactor at pressure of 1 bar.

The oxidation of m-xylene has been studied by Gaïl and Dagaut [104] using a JSR at atmospheric pressure, over a wide range of equivalence ratios (0.5 to 1.5) and temperatures (900-1400 K). A kinetic model of m-xylene was derived and used to analyze the results. The study done by Gaïl and Dagaut showed that the reactivity of m-xylene is similar, but slightly lower, to that of p-xylene under the evaluated conditions. This reactivity difference between the two isomers was studied in more detail in [31] by using a RCM at higher pressures, as shown previously in Figure 9. The results showed that o-xylene has the highest reactivity between all the isomers of xylene. Additional studies of m-xylene were performed using a shock tube to determine the ignition delay [94, 105, 106], species profile from reactors [107], and laminar flame speed [108]. From the kinetic model for toluene, a kinetic model for m-xylene was developed in [106] and the model predictions were compared to the experimental data from the shock tube. Narayanaswamy et al. [109] developed detailed model for toluene, styrene, ethylbenzene, 1,3-dimethylbenzene (m-xylene), and 1-methylnaphthalene. The model was validated against plug-flow reactor data for ignition delay times, species profiles from shock tube experiments, and laminar burning velocities.

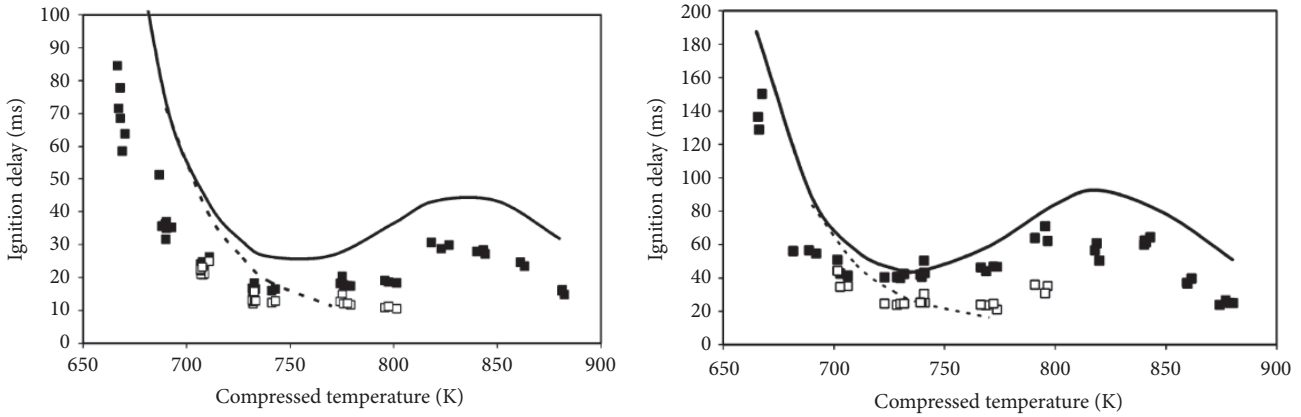

Figure 6: Ignition delay times of cyclohexane at equivalence ratio of 1 in the pressure range of 7-9 atm (right), 11-14 atm (left) from a RCM investigation and model-predicted values (line) at 8 atm (left) and 12.5 atm (right). Open symbols and dashed line correspond to cool flame delay times. Picture is adopted from Silke et al. [26].

Table 7: The major aromatic components in Chinese finished gasoline, Japanese finished regular gasoline, and Japanese finished premium gasoline, adopted from [135]. Part of the table is reported for component weight fraction higher than 0.9%.

Compound name	Japanese finished premium gasoline (Wt%)	Japanese finished regular gasoline (Wt%)	Chinese finished gasoline (Wt%)
Toluene (C_7H_8)	22.345	5.744	3.550
m-xylene (C_8H_{10})	0.765	1.487	2.669
o-xylene (C_8H_{10})	0.174	0.697	1.444
p-xylene(C_8H_{10})	0.439	0.582	0.951
1-methyl-4-ethylbenzene (C_9H_{12})	1.094	0.630	0.411
1-methyl-3-ethylbenzene (C_9H_{12})	2.396	1.463	1.108
1-methyl-2-ethylbenzene (C_9H_{12})	1.043	0.555	0.390
1,2,4-trimethylbenzene (C_9H_{12})	3.932	2.185	1.954
1,2,3-trimethylbenzene (C_9H_{12})	0.963	0.516	0.484
ethylbenzene (C_8H_{10})	0.828	0.714	0.909
1,3,5-trimethylbenzene (C_9H_{12})	0.938	0.577	0.521

2.6. Oxygenated Component. Studying the oxidation of ethanol is crucial in predicting gasoline combustion since approximately 10% of US gasoline by volume (E10) contains ethanol [21], as required by current US federal and state urban air quality standards [110]. With a RON/MON of 116.3/101.4, the combustion characteristics of ethanol have been studied extensively using low pressure shock tubes [111–114], high pressure shock tubes [115–118], RCMs [118–121], burners [113, 114, 122], turbulent flow reactors [113, 114, 123], and a JSR [114]. Kinetic models of ethanol have been studied and developed by [4, 110, 112, 115, 118, 119, 121, 123–128]. In addition, the combustion characteristics of mixtures of ethanol and gasoline were discussed by [124, 129]. Zyada and Samimi [121] developed an ethanol kinetic model using an automated reaction mechanism generator (RMG) and validated the mechanism against measured ignition delay times, laminar flame speeds, and species concentrations data. The new mechanism simulated the combustion of ethanol very well. Marinov [110] developed a detailed model for the combustion of ethanol and validated it against a variety of experimental datasets, such as laminar flame speed data (obtained from a constant-volume bomb and counter-flow twin-flame), ignition delay data behind a reflected shock wave, and ethanol oxidation product profiles from a jet-stirred and turbulent flow reactor. Good agreement was found in modeling of the datasets obtained from the five different experimental systems. Cancino et al. [115, 130] studied and developed an ethanol kinetic model using high pressure shock tube data. They used a few submechanisms from [110, 131] and found an ignition delay correlation for ethanol. The model was then used in ethanol-gasoline fuel surrogates by mixing the model of ethanol with other hydrocarbon models. They also found out the pressure sensitivity of ethanol is -0.83 [115] which is lower than gasoline fuel (-1.06). It should be mentioned that Heufer and Olivier [116] found -0.77 to be the pressure sensitivity. The model of Cancino et al. [130] still needed improvements as the final model underestimated the ignition delay data for pure ethanol and all combinations of components that featured ethanol. Olm et al. [128] recently developed a detailed mechanism by

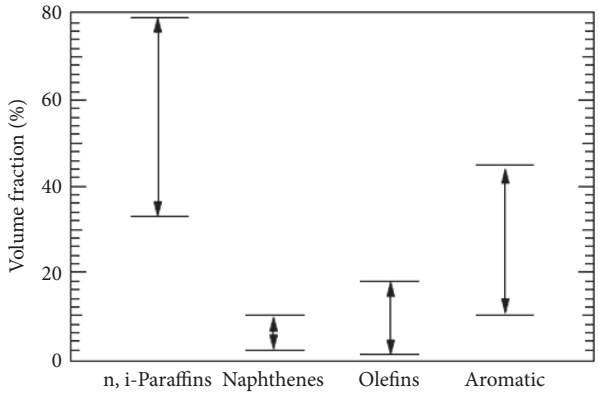

Figure 7: Approximate ranges of paraffins, naphthenes, olefins, and aromatics in commercial US gasoline. Figure is adopted from Pitz et al. [26].

optimizing 44 Arrhenius parameters of 14 crucial elementary reactions in the detailed mechanism created by Saxena and Williams [125]. They validated the model using ignition delay, species concentration, and flame velocity measurements. It was shown that the optimized mechanism provides better predictions of available experimental data. Lee et al. [118] took the ethanol mechanism of Li et al. [132] and improved it using parameters found in literature. They validated it against experimental data from [115, 116] and from extensive experimentation using a shock tube (at 80 bar) and RCM (at 40 bar) to cover temperatures between 700 to 1000 K. Metcalf et al. [127] created the AramcoMech 1.3 mechanism for C_1-C_2 hydrocarbons (methane, ethane, ethylene, acetylene, methanol, acetaldehyde, and ethanol). They changed the rate constant and thermodynamics properties (enthalpy and entropy) of significant reactions they found in the literature for the hydrocarbons species based on a sensitivity analysis. The model of Metcalf et al. [127] predicts the ignition delay well and performs better than the models of [110, 132]. Barraza-Botet et al. [120] studied ethanol for the stoichiometric ethanol/air mixture with dilutions. They used this data to validate the model of [133, 134], which is a version of AramcoMech, for C_1-C_3 hydrocarbons and oxygenated species oxidation. They used the ignition delay and speciation data from their RCM experiments to modify the rate constants of important hydrogen abstraction reactions of ethanol.

3. Gasoline Surrogates Review

Some gasoline surrogates from literature are modeled and compared with available experimental data in this section. These fuel surrogates were selected for review as the ignition delay time was one of the primary targets for the surrogate development. Primary Reference Fuel or PRF (mixture of iso-octane and n-heptane) is studied initially to address the deficiency of this surrogate model and highlight the necessity of further gasoline surrogate refinement through the addition of other components to the surrogate mixture. Ten surrogates with more complexity than PRF are reviewed and the ignition delays and other properties are modeled and compared with

Table 8: RD387 physical and chemical properties.

	RD387 [23]	RD387 [10]
Saturates (liq. volume %) n-/iso-/cyclo-alkanes	67.8 (9.5/42.3/16)	-
Alkenes (liq. volume %)	4.7	-
Aromatics (liq. volume %)	26.4	-
H/C ratio	1.869	1.85
RON/MON	91/82.7	-
Specific gravity @15.56°C (gr/cm^3)	0.7456	-
Net heating value (MJ/kg)	43.152	-

experiments. All of the ignition delay times are modeled using the mechanism of [19] at lean fuel/air conditions, which is similar to the operating conditions seen in HCCI engines. The autoignition of oxygenated gasoline fuels, such as E10, was not experimentally studied at the time of writing; yet most of the fuel surrogates were developed by adding ethanol to PRF and Toluene Reference Fuel (TRF) surrogates, such as the surrogate of [4]. Therefore, the oxygenated surrogates were not studied in the current review due to a lack of experimental data. In the following section, properties of RD387 (in addition to experimental data) are used as a representative of gasoline fuel. Table 8 shows some important properties of RD387. In this work, RD387 is the nonoxygenated gasoline and the terms shall be used interchangeably. Ignition delay measurements for gasoline RD387 have been reported by Kukkadapu et al. [23] using a RCM and Gauthier et al. [10] using a shock tube. Kukkadapu et al. [23] measured the ignition delay of the nonoxygenated gasoline at a wide range of compressed pressures (20 and 40 bars), equivalence ratios (0.3, 0.5, and 1), and compressed temperatures (667K to 950K). Gauthier et al. [10] measured the ignition delay times of RD387 using a shock tube at lean, stoichiometric, and rich conditions (equivalence ratio = 0.5, 1.0, 2.0), two pressure ranges (15–25 and 45–60 atm), temperatures from 850 to 1280 K, and exhaust gas recirculation (EGR) loadings of 0%, 20%, and 30%. In this paper, RCM experiments are simulated using a zero-dimensional model that accounts for the finite compression time and heat loss to the walls. RCM calculations start at the initial conditions of the experiment and the mixture is compressed at the same rate indicated by the measured pressure profile. The heat loss characteristics are determined by interrogation of nonreacting and reacting RCM experiments in which the oxygen of the fuel-air mixture was replaced by nitrogen. In RCM and shock tube simulations the ignition delay times were defined as the time when OH mole fraction reaches its maximum value. Modeling calculations show that the ignition delay corresponding to the maximum OH concentration is equivalent to definitions based on pressure or pressure rise rate for both the highly exothermic shock tube and RCM environments considered here. The research octane and motor octane numbers (RON and MON) of surrogates are calculated using the nonlinear correlation of Ghosh et al. [136]. The determination of a distillation curve is accomplished by approximating the system as a series of flash equilibrium stages, which is equivalent to the

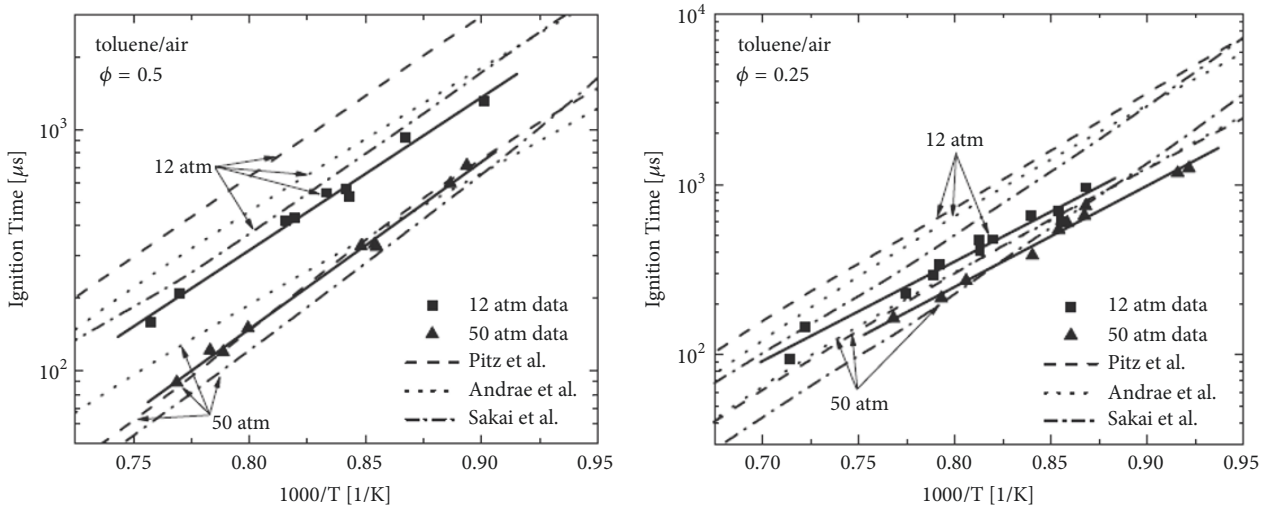

Figure 8: Ignition time measurements [27] for toluene/air mixtures at 12 and 50 atm at $\Phi = 0.5$ comparing the predictions of three kinetic mechanisms, Pitz et al. [28], Andrae et al. [29], and Sakai et al. [30]. Ignition times were scaled to 12 and 50 atm to account for slight deviations in reflected shock pressure by $P^{-0.50}$ as determined by regression analysis. Figure is adopted from Shen et al. [27].

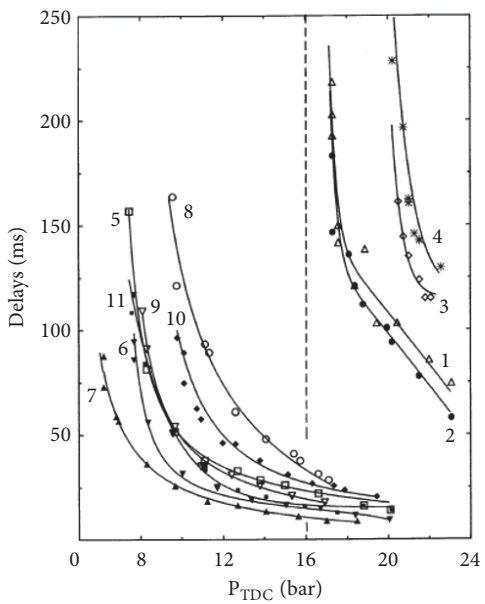

Figure 9: Autoignition delays of low alkylbenzenes around 900 K versus pressure at top dead center (TDC). Test at Φ=1, (O2)/(Inert) = 0.27 and T_{TDC}=907±6 K. Numbers correspond to the following: 1: toluene; 2: 1,3,5-trimethylbenzene; 3: p-xylene; 4: m-xylene; 5: o-xylene; 6: 1,2,3-trimethylbenzene; 7: ethyltoluene; 8: 1,2,4-trimethylbenzene; 9: n-propylbenzene; 10: ethylbenzene; 11: n-butylbenzene. Figure is adopted from Roubaud [31].

distillation curve measurement procedure outlined by ASTM D86. At each equilibrium stage, the saturated vapor pressure of each pure component is evaluated based on a DIPPR [137] correlation and the activity coefficient is calculated based on the UNIFAC [138] group interaction correlation. Ignition delay and distillation curve calculations are carried out using Chemkin-Pro [139] and Workbench packages [140].

Table 9: Composition and properties of PRF surrogate.

	PRF87
iso-alkanes (molar, %)	
iC_8H_{18}	86
n-alkanes (molar, %)	
nC_7H_{16}	14
Aromatics (molar, %)	
$C_6H_5CH_3$	0
H/C ratio	2.254
RON/MON	87/87
Specific gravity @15.56°C (gr/cm^3)	0.6892
Net heating value (MJ/kg)	44.64

Simulation of multicomponent gasoline surrogate models is studied in the next section.

3.1. Primary Reference Fuel Surrogate. The PRF surrogate with an octane number of 87 (PRF87) is the first to be evaluated. Details of the surrogate are shown in Table 9. PRF87's H/C ratio (2.254) is higher than RD387's (1.869), as shown in Tables 8 and 9, since both of the components in the PRF mixture (iso-octane and n-heptane) have H/C ratio of around 2.2. PRF has an initial boiling temperature of 99°C regardless of mixture composition (from the percentage of iso-octane with respect to n-heptane) and the distillation curve is nearly a straight line as shown in Figure 10. The PRF surrogate distillation curve does not follow the gasoline distillation curve. The total and first-stage ignition delays of PRF87 are shown in Figures 11 and 12. The performance of the surrogate at temperatures higher than 800 K is satisfactory and the surrogate ignition delay behavior in the NTC region is close to that of RD387. The surrogate first-stage ignition delay shows the same behavior as gasoline (a decrease as

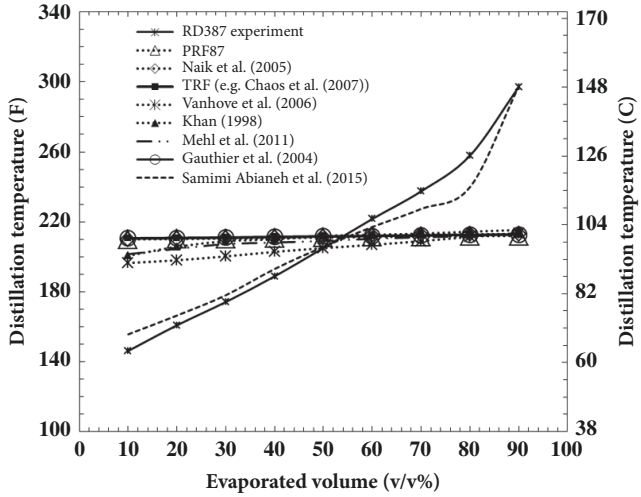

Figure 10: Distillation curves for gasoline RD387 fuel and surrogates. The simulated distillation curves are based on the staged equilibrium distillation model.

Table 10: Composition and properties of Chaos et al. [12], Vanhove et al. [11], and Khan [32] surrogates.

	Chaos et al. [12]	Vanhove et al. [11]	Khan [32]
iso-alkanes (molar, %)			
iC_8H_{18}	68.7	47	40.6
n-alkanes (molar, %)			
nC_7H_{16}	10.3	0	13
cyclo-alkanes (molar, %)			
C7H14	0	0	0
Aromatics (molar, %)			
$C_6H_5CH_3$	21	35	40.7
Olefins (molar, %)			
1-C_5H_{10}	0	0	5.7
1-C_6H_{12}	0	18	0
H/C ratio	2.0416	1.8409	1.8121
RON/MON	94.12/91.78	103.68/94.59	93.51/88.31
Specific gravity @15.56°C (gr/cm^3)	0.7152	0.7338	0.7421
Net heating value (MJ/kg)	43.94	43.44	43.19

temperature increases) but the surrogate first-stage ignition delay time is lower than that of gasoline. Samimi Abianeh et al. [19], Chaos et al. [12], Vanhove et al. [11], Khan [32], and others added some hydrocarbon components to the PRF surrogate to improve the total and first-stage ignition delay predictions, as will be discussed in the following sections.

3.2. Chaos et al. Surrogate. Chaos et al. [12] developed a three-component Toluene Reference Fuel (TRF) surrogate to represent gasoline's autoignition behavior. The surrogate mixture composition and properties are shown in Table 10 and distillation curve is shown in Figure 10. The H/C ratio and octane number of the surrogate are higher than those of gasoline (RD387), while the distillation curves of the TRF and PRF surrogates are identical and far from the distillation curve of gasoline. The surrogate model of Chaos et al. [12] was verified by using experimental data from a variable pressure flow reactor. The species mass fractions of carbon monoxide and dioxide, oxygen, and fuel components were modeled and measured during the autoignition process. The ignition delay of several surrogate mixtures was modeled and compared with shock tube experimental data to optimize the final surrogate. The final optimized surrogate was utilized for HCCI engine modeling to predict the pressure history, but the predicted results were not satisfactory. The ignition delay time comparisons are shown in Figures 13 and 14. The surrogate's ignition delay at 20 bar is in better agreement with gasoline's ignition delay at 40 bar. Ignition delay times in the NTC region and low temperatures for an equivalence ratio of 0.3 are higher than those found in the gasoline data. However, the first-stage ignition delay of the TRF surrogate is closer to the gasoline experiments than the PRF87 surrogate, as shown in Figures 13 and 14.

3.3. Vanhove et al. Surrogate. Vanhove et al. [11] studied the autoignition of five undiluted stoichiometric mixtures: n-heptane/toluene, iso-octane/toluene, iso-octane/1-hexene, 1-hexene/toluene, and iso-octane/1-hexene/toluene in a RCM for temperatures below 900 K. The first-stage ignition delay, total ignition delay, and some of the intermediated species were measured in their work. A gasoline surrogate was proposed with a mixture composition of iso-octane/1-hexene/toluene as shown in Table 10. The total ignition delay of Vanhove et al.'s gasoline surrogate is shown in Figure 13. The surrogate did not show first-stage autoignition at lean conditions. The octane number and total ignition delay of the surrogate are higher than the RD387 data as shown in Table 10 and Figure 13. The surrogate was mainly developed for European gasoline which has a higher octane number than US gasoline.

3.4. Khan Surrogate. Khan [32] formulated a surrogate mixture to have similar ratios of hydrocarbon groups, octane rating, and low and intermediate temperature reactivity as several industry standard fuels, such as Reference Fuel A (RFA) from the Auto/Oil Air Quality Improvement Research Program, indolene (the certification fuel), and a standard test fuel from Ford. The H/C ratio and octane number of the surrogate are close to RD387 as shown in Table 10. Lenhert et al. [141] investigated the reactivity behavior of the gasoline surrogate of Khan in a pressurized flow reactor over the low and intermediate temperature regime (600–800 K) at an elevated pressure (8 atm). Fuel species profiles as a function of reactor temperature were compared with experimental data to investigate and verify the surrogate performance in [141]. The total and first-stage ignition delay times of the surrogate are modeled and compared with those from experiments as shown in Figures 13 and 14. The total ignition delay behavior of Khan is close to Chaos et al. [12] and gasoline fuel; however, the low-temperature ignition delay times are overpredicted

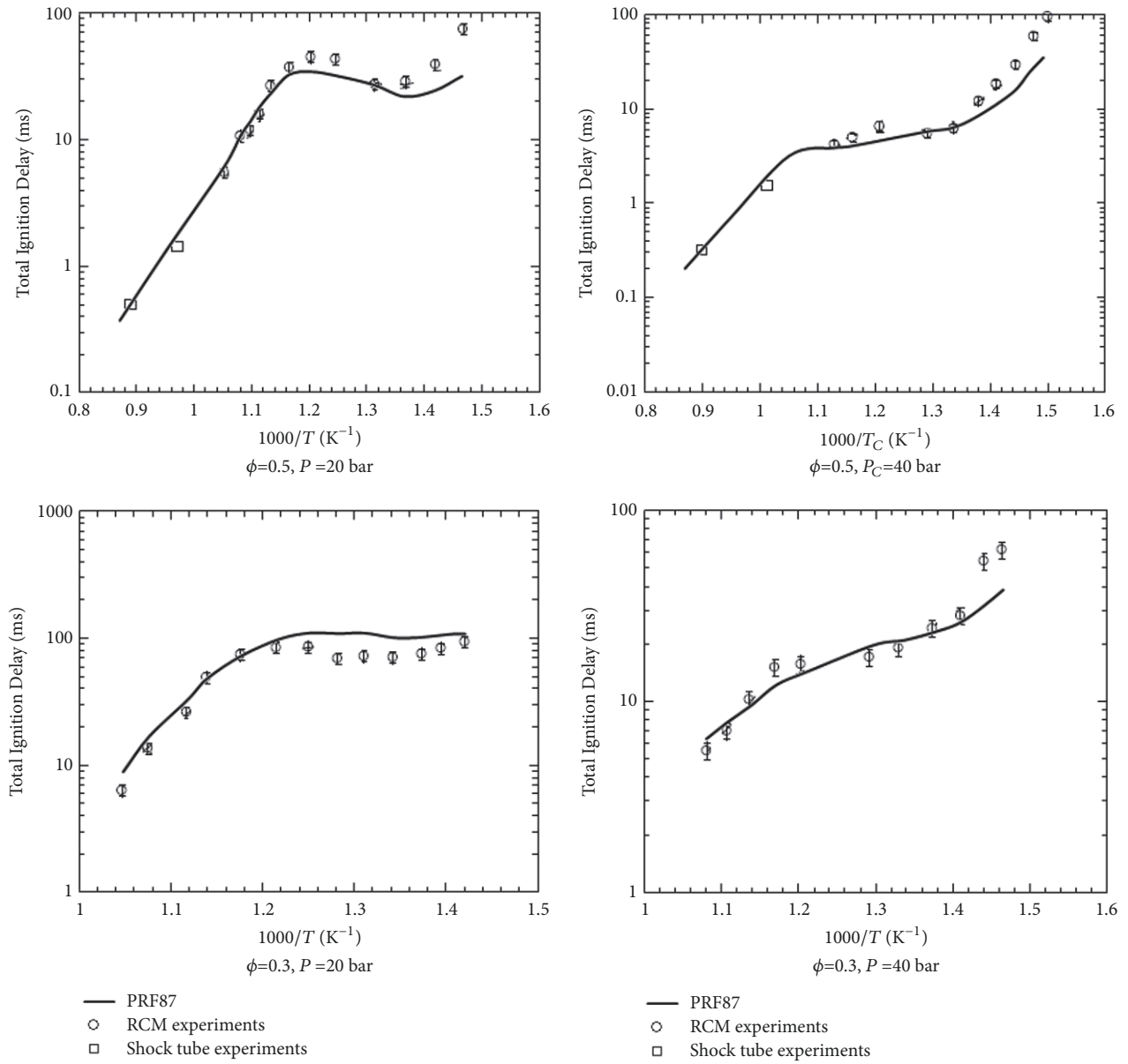

Figure 11: Comparison of RD387 experimental and simulated surrogate total ignition delay times. Experimental data is from Kukkadapu et al. [23] and Gauthier et al. [10]. Surrogate simulations were carried out using the PRF87 surrogate and mechanism model of Samimi Abianeh et al. [19]. Measured shock tube data are shown using □ at two approximate temperatures of 1000 K and 1100 K.

with respect to gasoline at very lean conditions (i.e., Φ=0.3). The first-stage ignition delay of the surrogate is in agreement with the gasoline data as shown in Figure 14.

3.5. Naik et al. Surrogate. Naik et al. [33] developed three surrogates for gasoline autoignition at lean conditions to model HCCI engine combustion. The surrogates' mixture compositions include iso-octane, n-heptane, 1-pentene, toluene, and methyl-cyclohexane which represent all the hydrocarbon groups in nonoxygenated gasoline fuel. The methodology for surrogate development was not discussed and the results were evaluated by using HCCI engine combustion pressure history and shock tube data. The surrogates' composition is shown in Table 11. The second surrogate has closer physical and chemical properties (octane number, heating value, and ignition delay) to gasoline than the other two surrogates. Only one distillation curve from the study is shown in Figure 10 since all three surrogates have identical distillation curve; none of them can accurately represent the distillation curve of gasoline. The total and first-stage ignition delay times of the three surrogates are compared with RD387 ignition delay data as shown in Figures 15 and 16. The total ignition delay time of the second mixture is very close to the experimental data, while the first-stage ignition delay times of mixtures 1 and 2 are similar to that of gasoline.

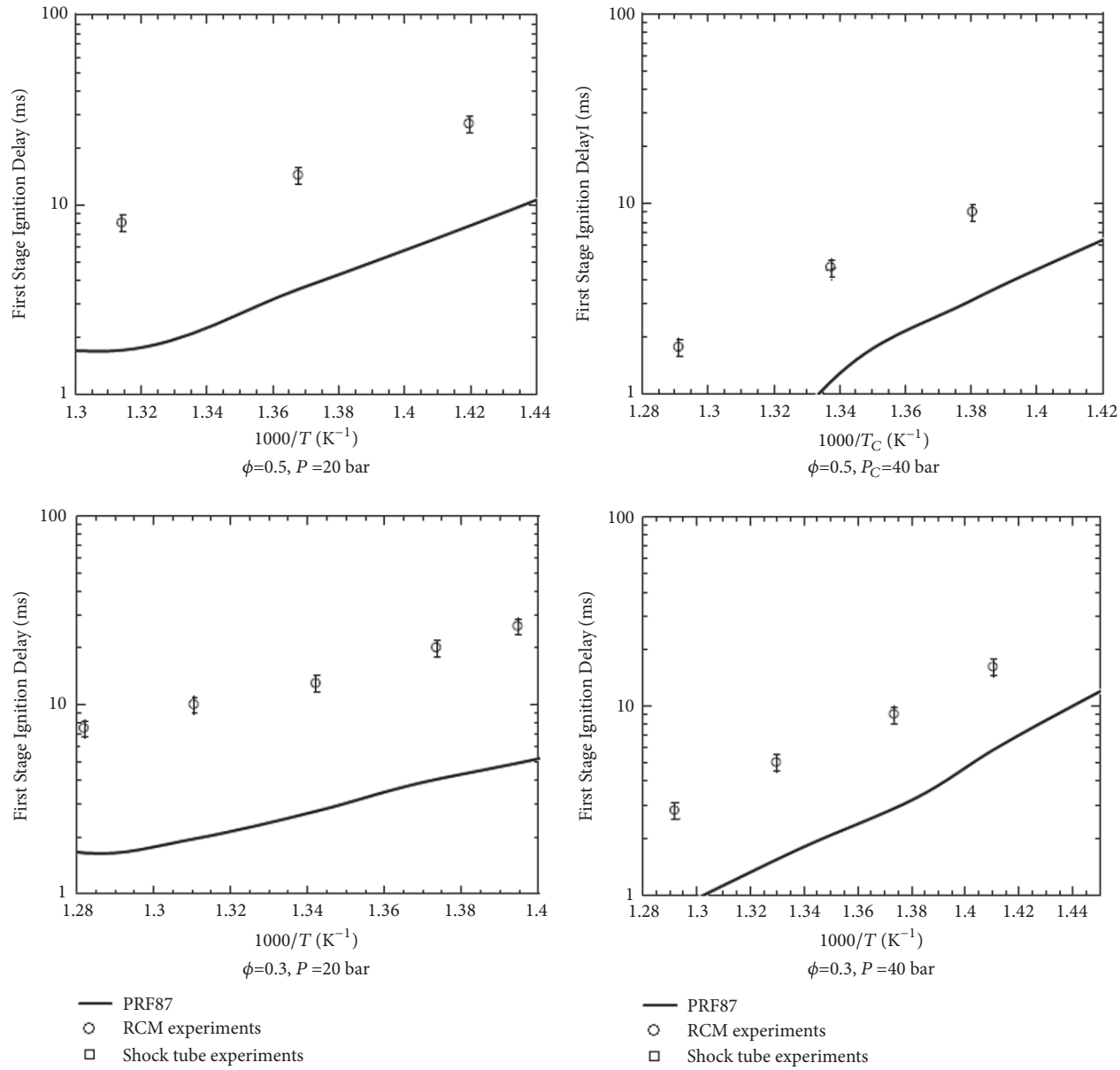

Figure 12: Comparison of experimental and simulated first-stage ignition delay times. Experimental data is from Kukkadapu et al. [23]. Surrogate simulations were carried out using the PRF87 surrogate and mechanism model of Samimi Abianeh et al. [19].

3.6. Mehl et al. Surrogate. Mehl et al. [13] formulated a four-component surrogate comprising iso-octane, n-heptane, toluene, and 2-pentene as shown in Table 12, which was found to emulate the laminar flame speed and ignition delay time of the target gasoline (RD387) to a good level of agreement. The distillation curve of the surrogate is shown in Figure 10 and does not follow the distillation curve of gasoline. The mechanism for the surrogate was developed by discriminating the species' detailed kinetic mechanism starting from the detailed mechanism of PRF. The gasoline surrogate was modeled at RCM and shock tube conditions and compared with RD387 experimental data of [19, 23]. This comparison study for total and first ignition delays is repeated and shown in Figures 17 and 18. The surrogate ignition delay is higher than gasoline's in the NTC region for an equivalence ratio of 0.3, as shown in Figure 17. However, the first-stage ignition delay times predicted the values and trend of gasoline's ignition delay well enough, as shown in Figure 18. The overall ignition delay of the surrogate is almost identical to Naik et al.'s [33] second surrogate ignition delay, both of which are close to gasoline's ignition delay. The surrogate and mechanism of Mehl et al. [13] should be verified experimentally since the surrogate was not experimentally validated unlike previously mentioned surrogates, such as PRF or TRF.

3.7. Gauthier et al. Surrogate. Gauthier et al. [10] studied the autoignition characteristics of n-heptane/air, gasoline/air

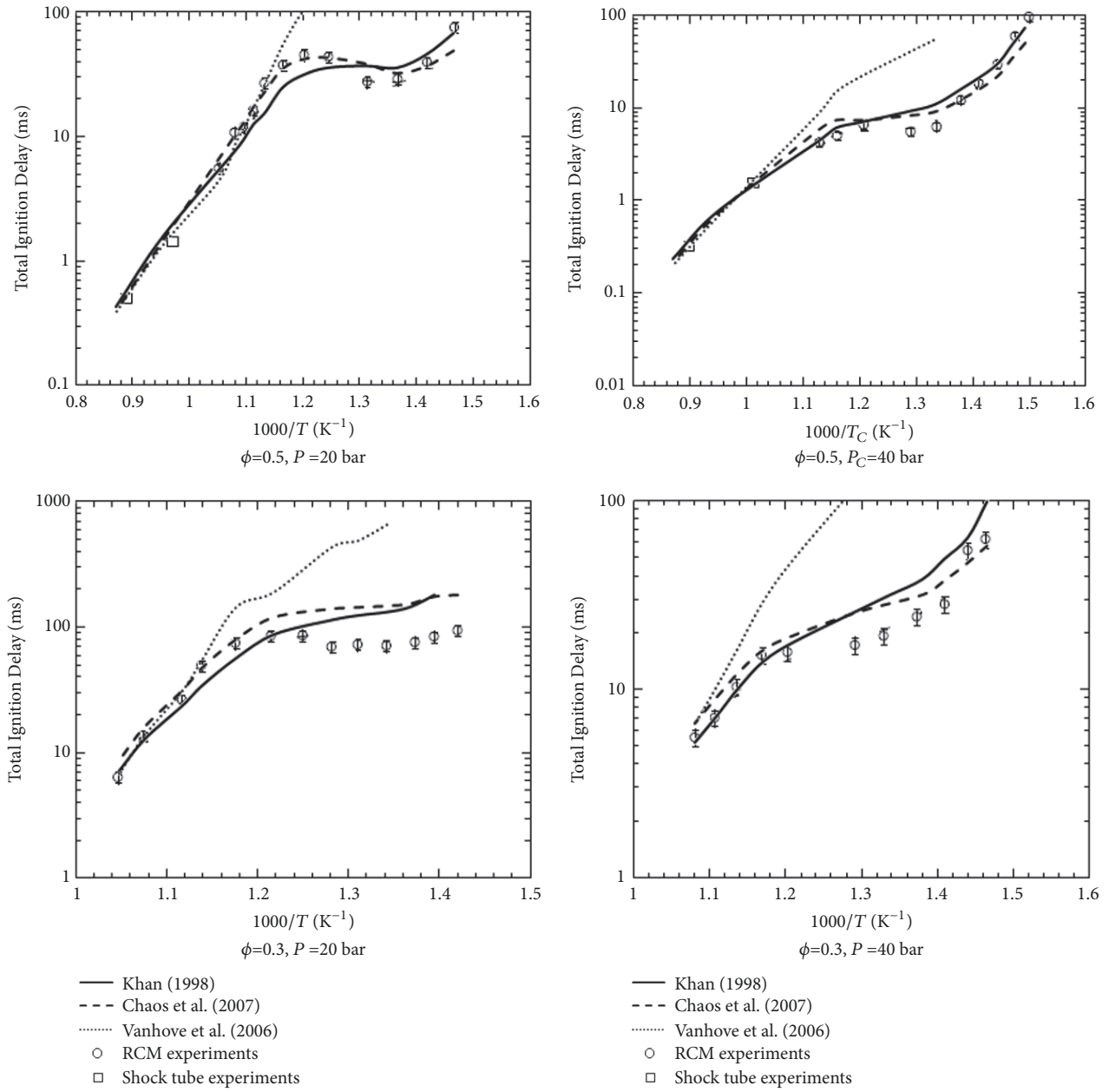

Figure 13: Comparison of RD387 experimental and simulated surrogate total ignition delay times. Experimental data is from Kukkadapu et al. [23] and Gauthier et al. [10]. Surrogate simulations were carried out using Khan [32], Chaos et al. [12], and Vanhove et al. [11] surrogates using the mechanism of Samimi Abianeh et al. [19]. Measured shock tube data are shown using □ at two approximate temperatures of 1000 K and 1100 K.

and two ternary gasoline surrogate/air mixtures by using a shock tube in a high pressure, low-temperature regime similar to conditions in a HCCI engine. Two ternary component gasoline surrogates for RD387 were developed by considering the gasoline ignition delay times as shown in Table 12. The surrogates' ignition delays were validated for temperatures between 850 K and 1250 K, pressures between 15 atm and 60 atm, equivalence ratios of 0.5, 1.0, and 2.0, and exhaust gas recirculating loadings from 0 to 30% using the shock tube. As shown in Table 12, the H/C ratio of the surrogates is not close to that of gasoline RD387. The distillation curve of the surrogate is shown in Figure 10 and does not follow the gasoline distillation curve. There is no significant difference between the two surrogates' ignition delay times as shown in Figures 17 and 18. By carefully examining these results, the following two conclusions can be realized: (1) small variations in octane number (±2) or H/C ratio (±4%) do not affect the ignition delay times and (2) the octane number and/or H/C ratio are more important than the mixture composition for developing a surrogate since the toluene mass fraction in the examined mixtures varied 33% between the two surrogates with negligible impact

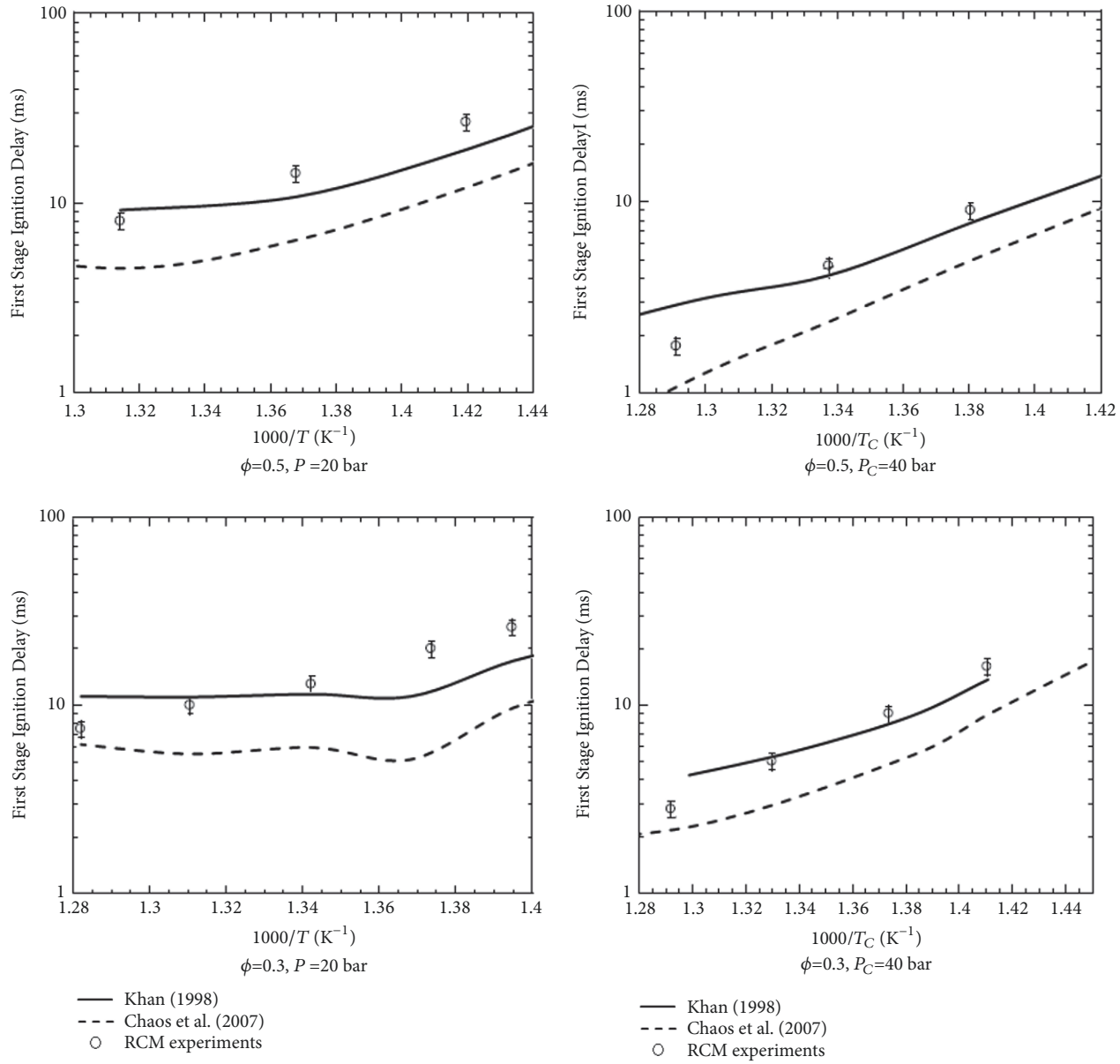

Figure 14: Comparison of experimental and simulated first-stage ignition delay times. Experimental data is from Kukkadapu et al. [23]. Surrogate simulations were carried out using Khan [32] and Chaos et al. [12] surrogates using the mechanism of Samimi Abianeh et al. [19].

to the ignition delay times. The ignition delay behaviors of Gauthier et al. [10] and Chaos et al. [12] (Figures 13 and 14) are almost identical and are close to the gasoline ignition delay data.

3.8. Samimi Abianeh et al. Surrogate. Samimi Abianeh et al. [19] developed a methodology for the formulation of a gasoline surrogate based on the essential physical and chemical properties of the target gasoline fuel. Using the proposed procedure, a surrogate with seven components was identified to emulate the physical and chemical characteristics of a real nonoxygenated gasoline fuel, RD387. A surrogate kinetic mechanism was developed by combining available detailed kinetic mechanisms from the Lawrence Livermore National Laboratory library [142]. Surrogate mixture composition was first defined by seeking a best fit to the primary targets utilizing a genetic algorithm and Powell minimization. The primary targets for the surrogate formulation were distillation curve, H/C ratio, octane numbers (RON and MON), heating value, and density of the gasoline fuel. Ignition delay time was defined as a secondary target since it requires calculation performed with a kinetic mechanism and is, hence, more computationally expensive to compute. The surrogate mixture composition is shown in Table 12 and distillation curve is shown in Figure 10. The H/C ratio, octane number, density, heating value, and distillation curve of the surrogate are similar to the gasoline RD387. None of the surrogates' distillation curves of the current study

Table 11: Composition and properties of Naik et al. [33] surrogates.

	mixture#1	mixture#2	mixture#3
iso-alkanes (molar, %)			
iC_8H_{18}	60	40	40
n-alkanes (molar, %)			
nC_7H_{16}	8	10	20
cyclo-alkanes (molar, %)			
c7h14	8	40	30
Aromatics (molar, %)			
$C_6H_5CH_3$	20	10	10
Olefins (molar, %)			
$1\text{-}C_5H_{10}$	4	0	0
H/C ratio	2.02	2.05	2.08
RON/MON	93.7/91.8	83.1/84.2	77.0/76.1
Specific gravity @15.56°C (gr/cm^3)	0.7185	0.7295	0.7214
Net heating value (MJ/kg)	43.9	43.94	44.02

Table 12: Composition and properties of Mehl et al. [13], Gauthier et al. [10], and Samimi Abianeh et al. [19] surrogates (note: the total component mass fraction in Gauthier et al.'s surrogate #1 is 1.01 as was reported in [10]).

	Mehl et al. [13]	Gauthier et al. [10], Mixture#1	Gauthier et al. [10], Mixture#2	Samimi Abianeh et al. [19]
iso-alkanes (molar, %)				
iC_5H_{12}	0	0	0	10.1
iC_6H_{14}	0	0	0	8.87
iC_8H_{18}	48.8	56	63	23.4
n-alkanes (molar, %)				
nC_5H_{12}	0	0	0	7.32
nC_7H_{16}	15.3	17	17	0
$nC_{12}H_{26}$	0	0	0	5.17
cyclo-alkanes (molar, %)				
c7h14	0	0	0	0
Aromatics (molar, %)				
$C_6H_5CH_3$	30.6	28	20	35.5
Olefins (molar, %)				
$2\text{-}C_5H_{10}$	5.3	0	0	9.66
H/C ratio	1.926	1.9718	2.0524	1.849
RON/MON	89.5/85.7	88.95/85.81	87.42/85.22	88.8/84.5
Specific gravity @15.56°C (gr/cm^3)	0.7272	0.7239	0.7135	0.7275
Net heating value (MJ/kg)	43.57	43.69	43.96	43.40

match the gasoline data except for the surrogate developed by Samimi Abianeh et al. The surrogate reproduces the physical properties of gasoline better than the other surrogates studied in this work. The ignition delay of the surrogate is shown in Figures 17 and 18. The total ignition delay is close to the gasoline ignition delay data, with the NTC region being well reproduced. The first-stage ignition delay of the surrogate has approximately the same value and trend as the gasoline fuel as shown in Figure 18. Samimi Abianeh et al.'s [19] surrogate includes a range of hydrocarbons from C_5 to C_{12} which covers the gasoline boiling temperature from 60°C to 150°C. The surrogate and mechanism need to be verified experimentally by a shock tube and a RCM.

To investigate the performance of the surrogate and kinetic model, the modeled laminar flame speed of several discussed gasoline surrogates and measured gasoline fuel are shown in Figure 19. Laminar flame speed measurements for European standard commercial gasoline (EN 228) with a

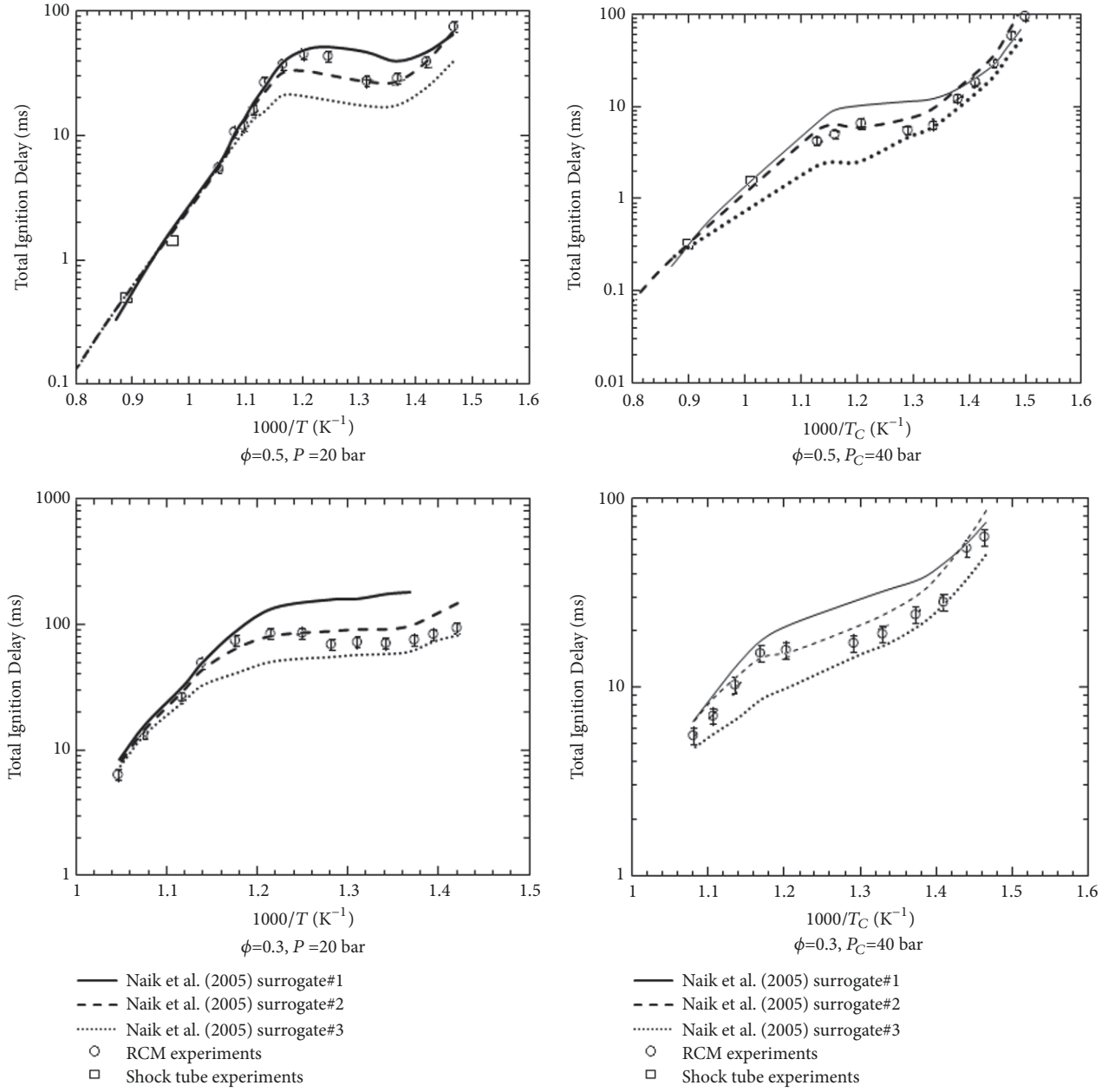

Figure 15: Comparison of RD387 experimental and simulated surrogate total ignition delay times. Experimental data is from Kukkadapu et al. [23] and Gauthier et al. [10]. Surrogate simulations were carried out using Naik et al. [33] surrogates using the mechanism of Samimi Abianeh et al. [19]. Measured shock tube data are shown using □ at two approximate temperatures of 1000 K and 1100 K.

RON/MON of 95/85 were performed by Jerzembeck et al. [34] using a constant-volume bomb under engine-relevant conditions. Although the composition and physical properties of the EN 228 gasoline were not reported, they are not expected to be the same as gasoline RD387 because EN 228 typically contains ethanol or other oxygenates at ~5% by liquid volume fraction. Regardless of the significant difference between the octane numbers of these surrogates (from 87 to 94), their modeled laminar flame speeds are similar and within the uncertainties of the measured data. At lean conditions, the modeled laminar flame speeds of all of the modeled surrogates are the same and the peak laminar flame speed occurs at an equivalence ratio of about 1.05; this value is 1.1 for measured data. There is a good agreement between simulations and experiments for stoichiometric and lean fuel-air mixtures but both models underpredict the measured laminar flame speeds for rich fuel-air mixtures at high pressure conditions (e.g., 20 and 25 bar). These discrepancies could be due to the surrogate mixtures, designed to emulate the nonoxygenated RD387 gasoline, not adequately representing the EN 228 gasoline, which may contain ethanol (around 5%) or other oxygenated components. The modeled

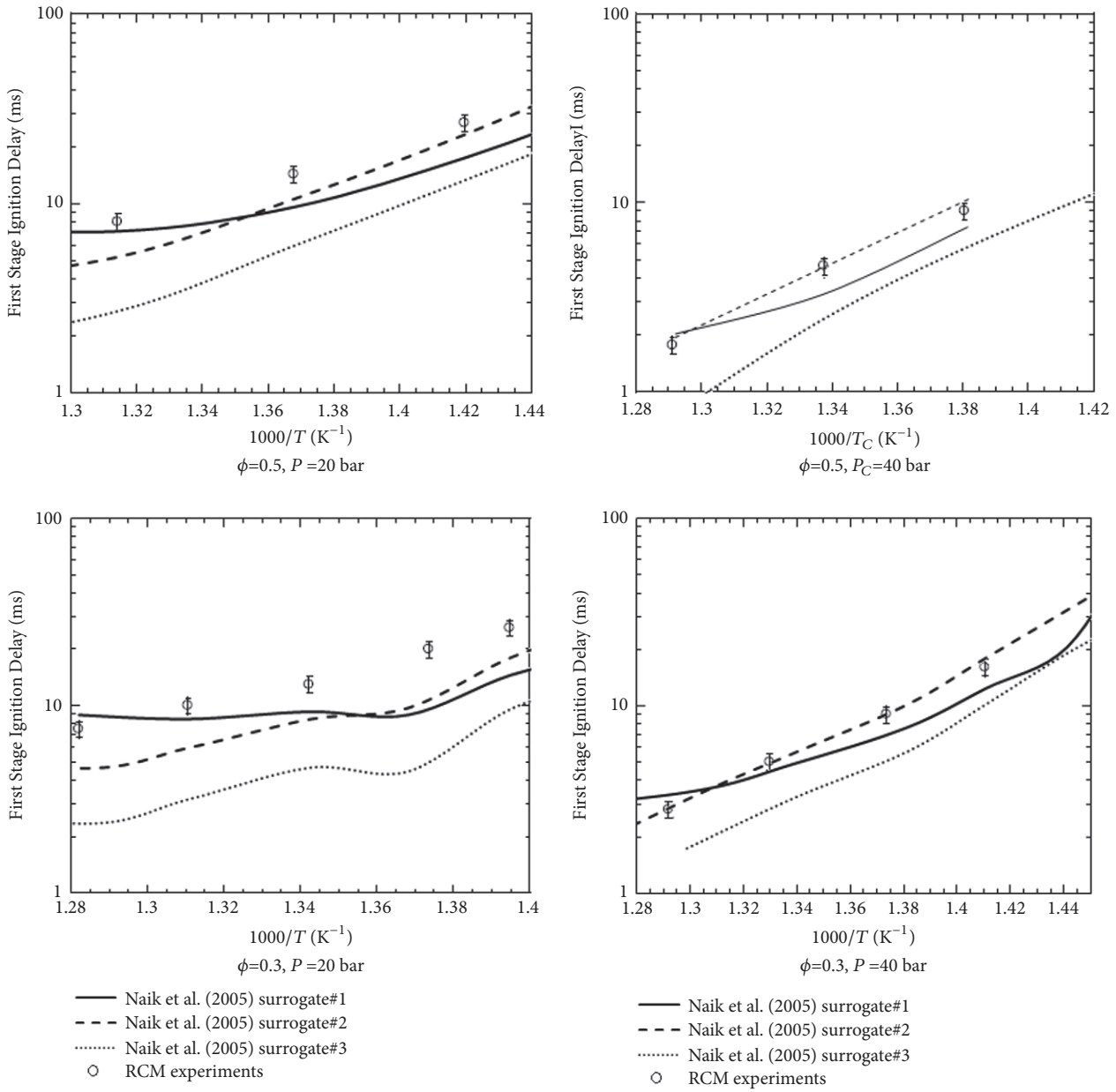

Figure 16: Comparison of experimental and simulated first-stage ignition delay times. Experimental data is from Kukkadapu et al. [23]. Surrogate simulations were carried out using Naik et al. [33] surrogates using the mechanism of Samimi Abianeh et al. [19].

laminar flame speed, even for PRF, is lower than what is reported in the modeled data of, e.g., Jerzembeck et al. [34] or Mehl et al. [13]. As was discussed in [19], this could be due to the removal of some important species and reactions during the mechanism reduction in the works of Jerzembeck et al. [34] and Mehl et al. [13].

3.9. Sensitivity Analysis. A sensitivity analysis has been conducted in order to identify the reactions within the current mechanism of [19] that influence ignition delay times under constant-volume conditions at an initial temperature of 720 K and 900 K, an initial pressure of 40 bar, and a fuel-air equivalence ratio of 1. These conditions were based on relevant RCM and advanced compression ignition engine data found in the literature. A first-order sensitivity analysis of gas temperature with respect to the reaction rate coefficient was carried out on the reaction rate coefficients of the mechanism. A temperature threshold of 0.1 was used to identify the major reactions. Since the sensitivity analysis is dependent on the surrogate components, the surrogate with several components of Samimi Abianeh et al. [19] was selected for sensitivity analysis. The results of the sensitivity analysis are shown in Figures 20 and 21. The results were produced by doubling the preexponential factor, A, for each important reaction rate coefficient in the kinetic mechanism, which was found using first-order sensitivity analysis in the

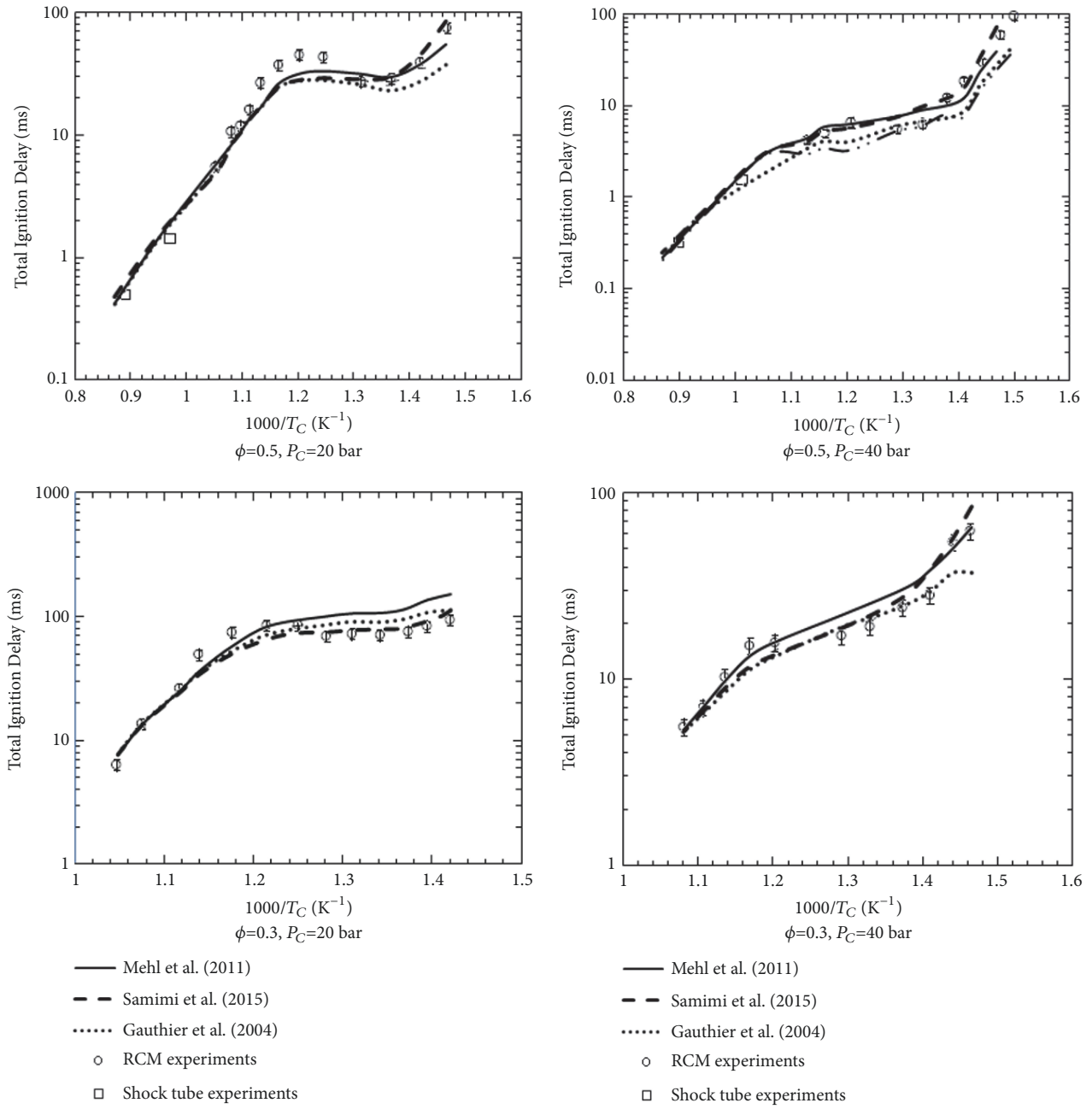

Figure 17: Comparison of RD387 experimental and simulated surrogate total ignition delay times. Experimental data is from Kukkadapu et al. [23] and Gauthier et al. [10]. Surrogate simulations were carried out using Mehl et al. [13], Gauither et al. [10], and Samimi Abianeh et al. [19] surrogates using the mechanism of Samimi Abianeh et al. [19]. Measured shock tube data are shown using □ at two approximate temperatures of 1000 K and 1100 K.

previous step. The sensitivity, defined as $S = (\tau(2A) - \tau(A))/\tau(A) \times 100$, was used to evaluate the influence of a particular rate constant on the total ignition delay. Negative sensitivity implies that a shorter ignition delay results from a doubling of the preexponential factor and that the reaction of interest promotes or accelerates the overall reaction rate. The summary of the sensitivity analysis is as follows:

(1) The iso-octane, n-dodecane, toluene, and 2-pentene decomposition reactions are the most dominant reactions among other reactions in the kinetic model at low to moderate temperatures. Changing their reaction coefficients significantly impacts the ignition delay.

(2) Iso-octane (iC_8H_{18}) decomposition reactions to C_8H_{17} isomers with attacking hydroxide change the ignition delay at low temperatures significantly.

(3) The H_2O_2 (+M) = 2OH (+M) reaction is more important at moderate temperatures. Given the activation

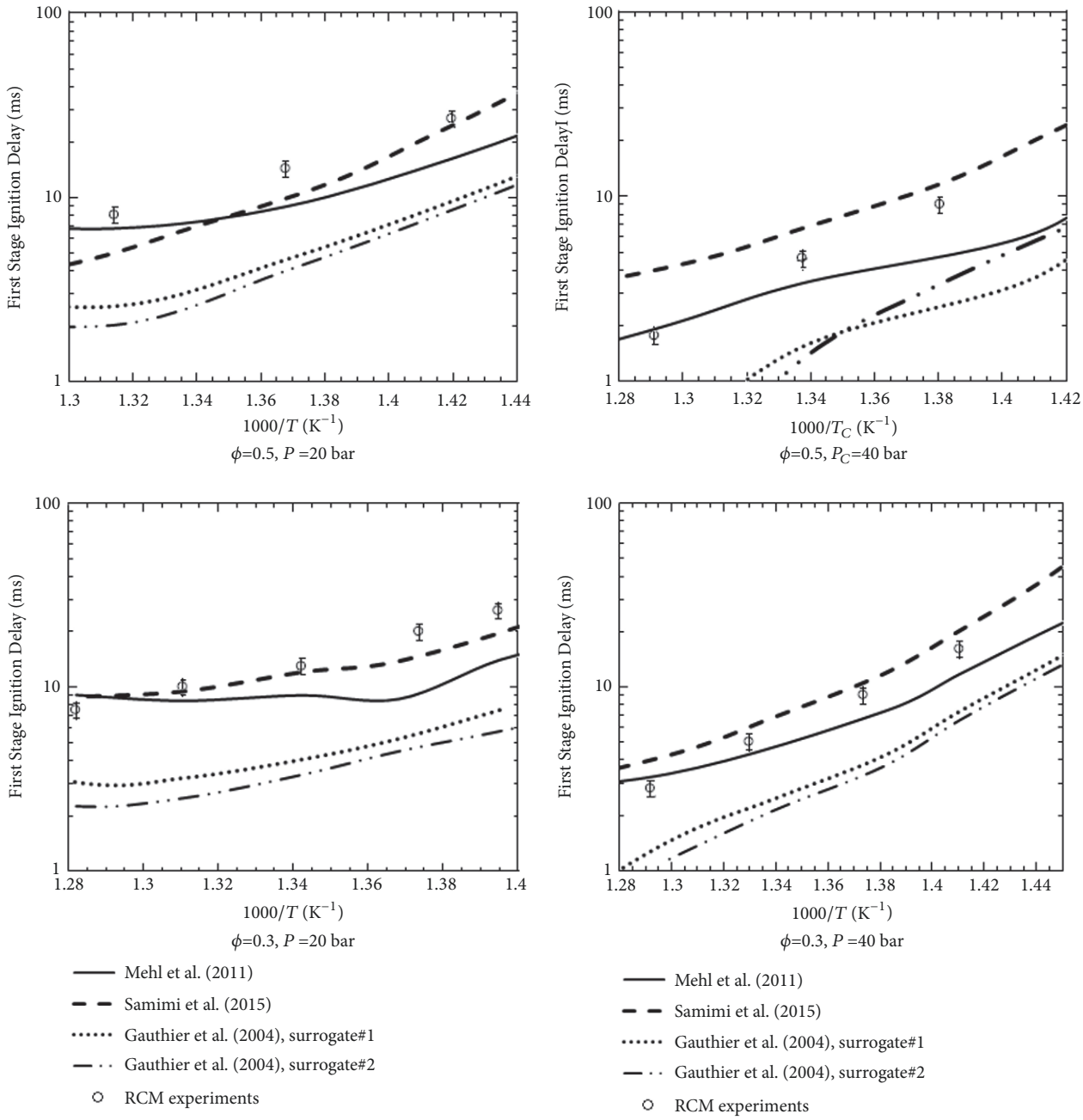

Figure 18: Comparison of experimental and simulated first-stage ignition delay times. Experimental data is from Kukkadapu et al. [23]. Surrogate simulations were carried out using Mehl et al. [13], Gauither et al. [10], and Samimi Abianeh et al. [19] surrogates using the mechanism of Samimi Abianeh et al. [19].

energy of H_2O_2 decomposition, this reaction only occurs at moderate to high temperatures and it changes the ignition delay significantly in this range.

(4) Dodecane ($nC_{12}H_{26}$) decomposition reactions to $C_{12}H_{25}$ are important at both low and moderate temperatures and it is due to the low activation energy of n-dodecane decomposition to $C_{12}H_{25}$ isomers. Doubling the reaction rates always reduces the ignition delay time regardless of isomers produced ($C_{12}H_{25}$).

(5) Toluene ($C_6H_5CH_3$) decomposition reactions (by attacking OH) alter the ignition delay at both low and moderate temperatures significantly. This could be caused by the very low activation energy of toluene.

(6) 2-pentene decomposition reactions to C_5H_9 by attacking the hydroxide are only important at low temperatures due to the low activation energy of the olefin. Increasing its rate of reaction will increase the ignition delay significantly.

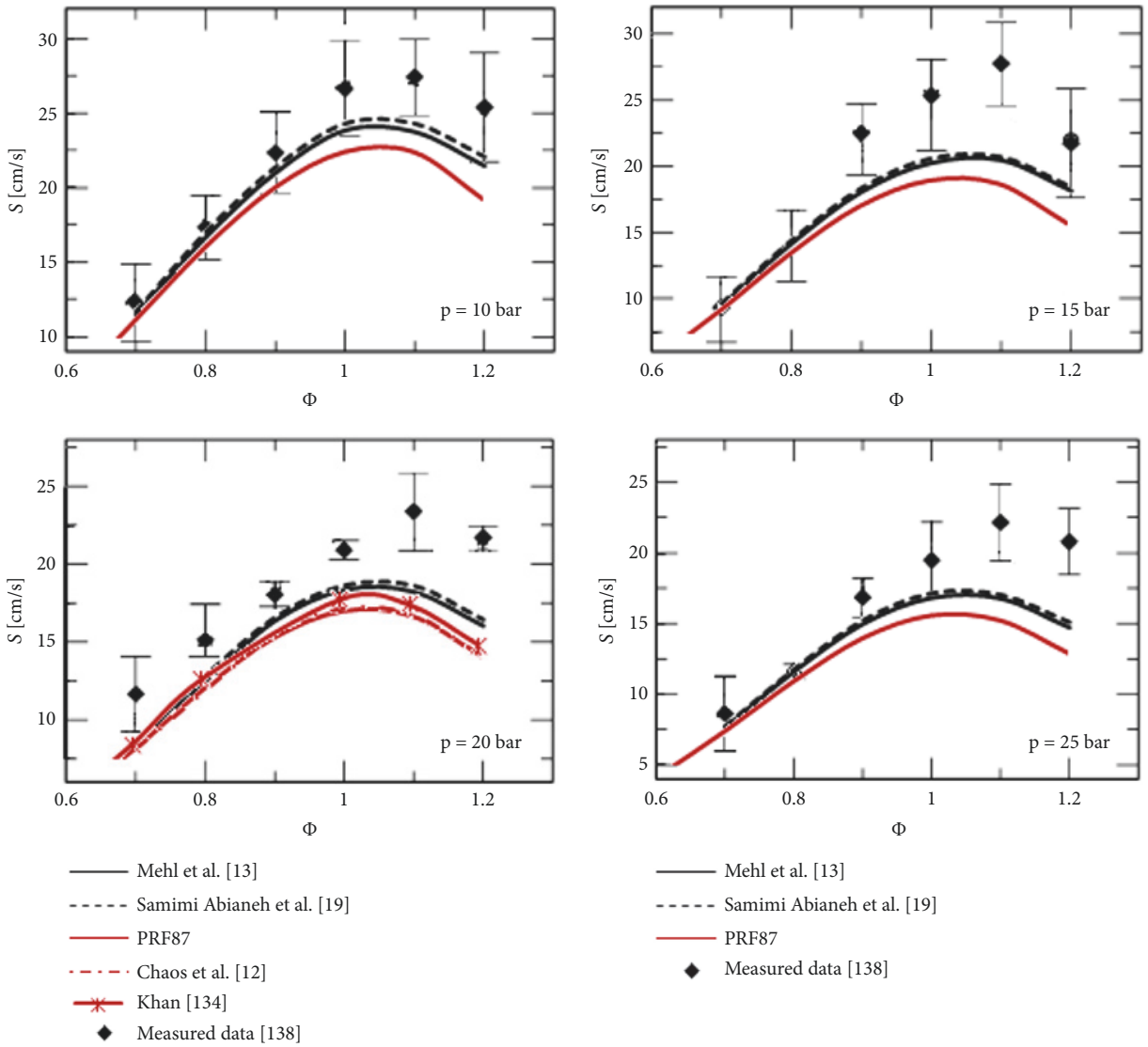

Figure 19: Comparison of measured gasoline laminar flame speeds and several modeled gasoline surrogates. Unburned gas temperature is 373 K and the oxygen mole fraction in air is 0.205 for both the experiments and simulations. Measured data is from Jerzembeck et al. [34].

4. Summary

The ultimate goal of developing a surrogate is to mimic all of the chemical and physical properties of a target fuel. There are two distinct and separate fuel surrogate development targets: physical properties (such as distillation curve, density, thermal conductivity, etc.) and combustion characteristics (such as ignition delay time and laminar flame speed). There is a scarce number of works which study the effect of the physical properties on the combustion characteristics or develop a gasoline surrogate to address both of these targets. Experimental data focuses on the combustion characteristics (e.g., the autoignition of gasoline) and is measured using shock tubes and RCMs. These methods neglect the effects of fuel's physical properties (such as density and distillation curve) and, therefore, lack necessary information.

Furthermore, the kinetic models of some of the major components in the gasoline fuel mixture, as discussed in this paper, are still unknown or not verified yet. Developing the kinetic models of these components can help develop a more reliable surrogate.

Some of the advanced gasoline surrogates and kinetic models were verified by comparing the modeled surrogate ignition delay with real gasoline data. These surrogates and their kinetic data should be verified by making and testing the surrogates experimentally to examine the reliability of the mechanism before comparing the results with the experimental data of gasoline.

None of the advanced, recently made surrogates that were previously discussed (i.e., those with the capability to mimic the ignition delay of gasoline over the whole range of temperatures, such as Mehl et al.'s [13] surrogate)

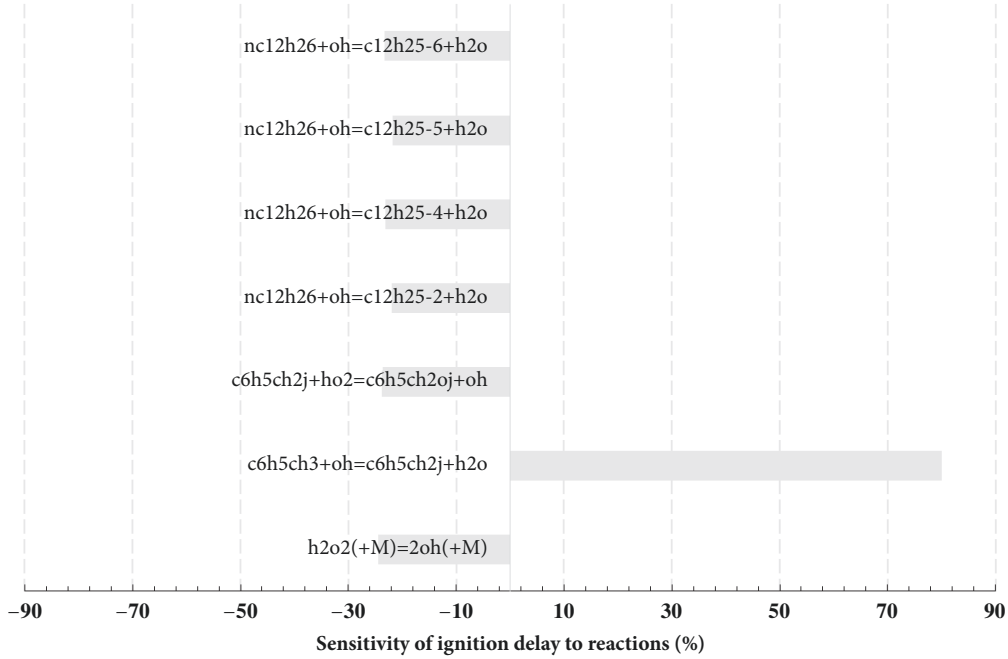

Figure 20: Sensitivity analysis for total ignition delays for prediction of ignition under constant-volume conditions at initial conditions of 900 K, 40 bar, and fuel-air equivalence ratio of 1.0.

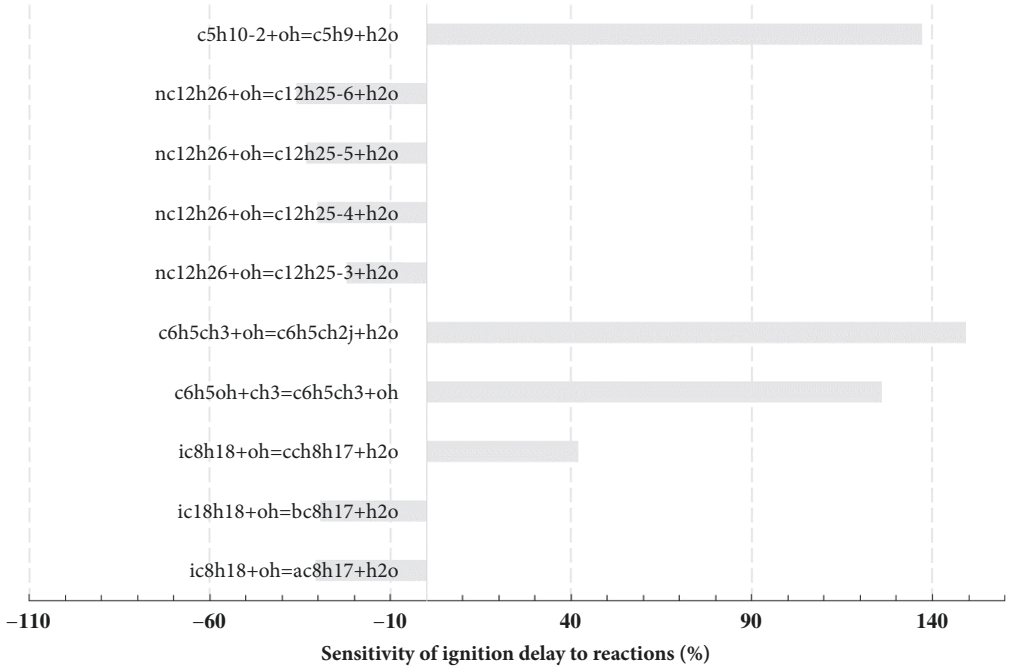

Figure 21: Sensitivity analysis for total ignition delays for prediction of ignition under constant-volume conditions at initial conditions of 715 K, 40 bar, and fuel-air equivalence ratio of 1.0.

were utilized in a CFD code for modeling the combustion of spark-ignition internal combustion engines except for the PRF and TRF surrogates. This type of modeling and comparison with experiments can show the effect of physical properties on spray penetration, autoignition, and the interaction between these properties in real engineering applications. The overall goal of these surrogates is to reduce the computational load of simulating the combustion of these fuels to expedite the development of advanced combustion systems.

The surrogates are developed depending on the working conditions (e.g., low temperatures versus high temperatures), application (e.g., SI engine versus HCCI engine), and target properties (e.g., distillation curve, density, etc.). As shown in the paper, the discussed surrogates' modeled laminar flame speed are approximately the same as measured data; however, their ignition delay times are significantly different. Thus, for SI engine applications in which the flame initiates via a spark, these surrogates could be utilized to model the combustion performance, e.g., location of peak pressure. However, if the objective is to predict knock in SI engines or the performance of HCCI engines, a surrogate which can mimic the ignition delay times of gasoline is needed.

Oxygenated gasoline fuels are the dominating transportation fuel in US. Despite this, the autoignition of these fuels (e.g., E10 and E85) has not been performed and the currently developed surrogates are deficient in their predictive ability. This is probably due to the addition of ethanol reaction pathways added to previous gasoline surrogates (e.g., TRF and PRF) without any analysis to the critical physical and chemical characteristics. Future work needs to be done to measure the characteristics of these oxygenated fuels and develop more accurate surrogate models.

Conflicts of Interest

The authors declare that they have no conflicts of interest.

Acknowledgments

Research was sponsored in-part by the Army Research Laboratory and was accomplished under Cooperative Agreement Number W911NF-18-2-0042. The views and conclusions contained in this document are those of the authors and should not be interpreted as representing the official policies, either expressed or implied, of the Army Research Laboratory or the US Government. The US Government is authorized to reproduce and distribute reprints for Government purposes notwithstanding any copyright notation herein.

References

[1] G.-S. Zhu and R. D. Reitz, "A model for high-pressure vaporization of droplets of complex liquid mixtures using continuous thermodynamics," *International Journal of Heat and Mass Transfer*, vol. 45, no. 3, pp. 495–507, 2001.

[2] Y. Ra and R. D. Reitz, "A vaporization model for discrete multicomponent fuel sprays," *International Journal of Multiphase Flow*, vol. 35, no. 2, pp. 101–117, 2009.

[3] S. S. Sazhin, A. Elwardany, P. A. Krutitskii et al., "A simplified model for bi-component droplet heating and evaporation," *International Journal of Heat and Mass Transfer*, vol. 53, no. 21-22, pp. 4495–4505, 2010.

[4] O. Samimi Abianeh, C. P. Chen, and S. Mahalingam, "Numerical modeling of multi-component fuel spray evaporation process," *International Journal of Heat and Mass Transfer*, vol. 69, pp. 44–53, 2014.

[5] T. Edwards and L. Q. Maurice, "Surrogate mixtures to represent complex aviation and rocket fuels," *Journal of Propulsion and Power*, vol. 17, no. 2, pp. 461–466, 2001.

[6] T. J. Bruno, "The Properties of S-8 and JP-10," Report prepared for Wright Laboratory Aero Propulsion Power Directorate under MIPR F4FBEY6346G001, 2007.

[7] S. L. Outcalt, A. Laesecke, and K. J. Brumback, "Thermophysical properties measurements of rocket propellants RP-1 and RP-2," *Journal of Propulsion and Power*, vol. 25, no. 5, pp. 1032–1040, 2009.

[8] M. L. Huber, E. W. Lemmon, and T. J. Bruno, "Surrogate mixture models for the thermophysical properties of aviation fuel Jet-A," *Energy & Fuels*, vol. 24, no. 6, pp. 3565–3571, 2010.

[9] O. S. Abianeh, C. P. Chen, and R. L. Cerro, "Batch distillation: The forward and inverse problems," *Industrial & Engineering Chemistry Research*, vol. 51, no. 38, pp. 12435–12448, 2012.

[10] B. M. Gauthier, D. F. Davidson, and R. K. Hanson, "Shock tube determination of ignition delay times in full-blend and surrogate fuel mixtures," *Combustion and Flame*, vol. 139, no. 4, pp. 300–311, 2004.

[11] G. Vanhove, G. Petit, and R. Minetti, "Experimental study of the kinetic interactions in the low-temperature autoignition of hydrocarbon binary mixtures and a surrogate fuel," *Combustion and Flame*, vol. 145, no. 3, pp. 521–532, 2006.

[12] M. Chaos, Z. Zhao, and A. Kazakov, "A PRF+ toluene surrogate fuel model for simulating gasoline kinetics," in *Proceedings of the 5th US Combustion Meeting*, pp. 25–28, San Diego, CA, USA, 2007.

[13] M. Mehl, J. Y. Chen, W. J. Pitz, S. M. Sarathy, and C. K. Westbrook, "An approach for formulating surrogates for gasoline with application toward a reduced surrogate mechanism for CFD engine modeling," *Energy & Fuels*, vol. 25, no. 11, pp. 5215–5223, 2011.

[14] C. J. Mueller, W. J. Cannella, T. J. Bruno et al., "Methodology for formulating diesel surrogate fuels with accurate compositional, ignition-quality, and volatility characteristics," *Energy & Fuels*, vol. 26, no. 6, pp. 3284–3303, 2012.

[15] C. J. Mueller, W. J. Cannella, and J. T. Bays, "Diesel surrogate fuels for engine testing and chemical-kinetic modeling: Compositions and properties," *Energy & Fuels*, vol. 30, no. 2, pp. 1445–1461, 2016.

[16] D. Kim, J. Martz, and A. Violi, "A surrogate for emulating the physical and chemical properties of conventional jet fuel," *Combustion and Flame*, vol. 161, no. 6, pp. 1489–1498, 2014.

[17] D. Kim, J. Martz, and A. Violi, "Effects of fuel physical properties on direct injection spray and ignition behavior," *Fuel*, vol. 180, pp. 481–496, 2016.

[18] A. Ahmed, G. Goteng, V. S. B. Shankar, K. Al-Qurashi, W. L. Roberts, and S. M. Sarathy, "A computational methodology for formulating gasoline surrogate fuels with accurate physical and chemical kinetic properties," *Fuel*, vol. 143, pp. 290–300, 2015.

[19] O. S. Abianeh, M. A. Oehlschlaeger, and C.-J. Sung, "A surrogate mixture and kinetic mechanism for emulating the evaporation and autoignition characteristics of gasoline fuel," *Combustion and Flame*, vol. 162, no. 10, pp. 3773–3784, 2015.

[20] D. Kang, V. Kalaskar, D. Kim, J. Martz, A. Violi, and A. Boehman, "Experimental study of autoignition characteristics of Jet-A surrogates and their validation in a motored engine and a constant-volume combustion chamber," *Fuel*, vol. 184, pp. 565–580, 2016.

[21] W. J. Pitz, C. V. Naik, T. Ní Mhaoldúin et al., "Modeling and experimental investigation of methylcyclohexane ignition in a rapid compression machine," *Proceedings of the Combustion Institute*, vol. 31, pp. 267–275, 2007.

[22] K. Owen and T. Coley, *Automotive Fuels Reference Book*, 1995.

[23] G. Kukkadapu, K. Kumar, C.-J. Sung, M. Mehl, and W. J. Pitz, "Experimental and surrogate modeling study of gasoline ignition in a rapid compression machine," *Combustion and Flame*, vol. 159, no. 10, pp. 3066–3078, 2012.

[24] C. K. Westbrook, W. J. Pitz, H. C. Curran, J. Boercker, and E. Kunrath, "Chemical kinetic modeling study of shock tube ignition of heptane isomers," *International Journal of Chemical Kinetics*, vol. 33, no. 12, pp. 868–877, 2001.

[25] H. J. Curran, P. Gaffuri, W. J. Pitz, and C. K. Westbrook, "A comprehensive modeling study of iso-octane oxidation," *Combustion and Flame*, vol. 129, no. 3, pp. 253–280, 2002.

[26] E. J. Silke, W. J. Pitz, C. K. Westbrook, and M. Ribaucour, "Detailed chemical kinetic modeling of cyclohexane oxidation," *The Journal of Physical Chemistry A*, vol. 111, no. 19, pp. 3761–3775, 2007.

[27] H.-P. S. Shen, J. Vanderover, and M. A. Oehlschlaeger, "A shock tube study of the auto-ignition of toluene/air mixtures at high pressures," *Proceedings of the Combustion Institute*, vol. 32, pp. 165–172, 2009.

[28] W. J. Pitz, R. Seiser, and J. W. Bozzelli, *Chemical Kinetic Characterization of Combustion Toluene*, Lawrence Livermore National Lab., CA, USA, 2001.

[29] J. C. G. Andrae, P. Björnbom, R. F. Cracknell, and G. T. Kalghatgi, "Autoignition of toluene reference fuels at high pressures modeled with detailed chemical kinetics," *Combustion and Flame*, vol. 149, no. 1-2, pp. 2–24, 2007.

[30] Y. Sakai, H. Ozawa, T. Ogura, A. Miyoshi, M. Koshi, and W. J. Pitz, "Effects of toluene addition to primary reference fuel at high temperature," *SAE Paper 2007-01-4104*, 2007.

[31] A. Roubaud, R. Minetti, and L. R. Sochet, "Oxidation and combustion of low alkylbenzenes at high pressure: Comparative reactivity and auto-ignition," *Combustion and Flame*, vol. 121, no. 3, pp. 535–541, 2000.

[32] R. Khan, "Oxidation of Industry Standard Fuels and Blends of Primary Reference Fuels in the Low Temperature and Negative Temperature Coefficient Regions," M.Sc. thesis, Drexel University, Philadelphia, PA, USA, 1998.

[33] C. V. Naik, W. J. Pitz, C. K. Westbrook et al., "Detailed chemical kinetic modeling of surrogate fuels for gasoline and application to an HCCI engine," *SAE Technical Paper 2005-01-3741*, 2005.

[34] S. Jerzembeck, N. Peters, P. Pepiot-Desjardins, and H. Pitsch, "Laminar burning velocities at high pressure for primary reference fuels and gasoline: Experimental and numerical investigation," *Combustion and Flame*, vol. 156, no. 2, pp. 292–301, 2009.

[35] C. B. Reuter, M. Lee, S. H. Won, and Y. Ju, "Study of the low-temperature reactivity of large n-alkanes through cool diffusion flame extinction," *Combustion and Flame*, vol. 179, pp. 23–32, 2017.

[36] F. L. Dryer, "Chemical kinetic and combustion characteristics of transportation fuels," *Proceedings of the Combustion Institute*, vol. 35, no. 1, pp. 117–144, 2015.

[37] M. Pelucchi, M. Bissoli, and C. Cavallotti, "Improved kinetic model of the low-temperature oxidation of n-heptane," *Energy and Fuels*, vol. 28, no. 11, pp. 7178–7193, 2014.

[38] L. Seidel, K. Moshammer, X. Wang, T. Zeuch, K. Kohse-Höinghaus, and F. Mauss, "Comprehensive kinetic modeling and experimental study of a fuel-rich, premixed n-heptane flame," *Combustion and Flame*, vol. 162, no. 5, pp. 2045–2058, 2015.

[39] K. Zhang, C. Banyon, J. Bugler et al., "An updated experimental and kinetic modeling study of n-heptane oxidation," *Combustion and Flame*, vol. 172, pp. 116–135, 2016.

[40] J. M. Simmie, "Detailed chemical kinetic models for the combustion of hydrocarbon fuels," *Progress in Energy and Combustion Science*, vol. 29, no. 6, pp. 599–634, 2003.

[41] C. K. Westbrook, W. J. Pitz, O. Herbinet, H. J. Curran, and E. J. Silke, "A comprehensive detailed chemical kinetic reaction mechanism for combustion of n-alkane hydrocarbons from n-octane to n-hexadecane," *Combustion and Flame*, vol. 156, no. 1, pp. 181–199, 2009.

[42] L. Cai, H. Pitsch, S. Y. Mohamed et al., "Optimized reaction mechanism rate rules for ignition of normal alkanes," *Combustion and Flame*, vol. 173, pp. 468–482, 2016.

[43] S. M. Sarathy, C. K. Westbrook, M. Mehl et al., "Comprehensive chemical kinetic modeling of the oxidation of 2-methylalkanes from C7 to C20," *Combustion and Flame*, vol. 158, no. 12, pp. 2338–2357, 2011.

[44] J. Bugler, K. P. Somers, E. J. Silke, and H. J. Curran, "Revisiting the kinetics and thermodynamics of the low-temperature oxidation pathways of alkanes: a case study of the three pentane isomers," *The Journal of Physical Chemistry A*, vol. 119, no. 28, pp. 7510–7527, 2015.

[45] P. A. Glaude, V. Warth, R. Fournet, F. Battin-Leclerc, G. Scacchi, and G. M. Côme, "Modeling of the oxidation of n-octane and n-decane using an automatic generation of mechanisms," *International Journal of Chemical Kinetics*, vol. 30, no. 12, pp. 949–959, 1998.

[46] M. Mehl, H. J. Curran, and W. J. Pitz, "Chemical kinetic modeling of component mixtures relevant to gasoline," in *Proceedings of the European Combustion Meeting*, Vienna, Austria, 2009.

[47] M. Mehl, W. J. Pitz, M. Sjöberg, and J. E. Dec, "Detailed kinetic modeling of low-temperature heat release for PRF fuels in an HCCI engine," *SAE Technical Papers*, 2009.

[48] N. Atef, G. Kukkadapu, S. Y. Mohamed et al., "A comprehensive iso-octane combustion model with improved thermochemistry and chemical kinetics," *Combustion and Flame*, vol. 178, pp. 111–134, 2017.

[49] C. K. Westbrook, W. J. Pitz, J. E. Boercker et al., "Detailed chemical kinetic reaction mechanisms for autoignition of isomers of heptane under rapid compression," *Proceedings of the Combustion Institute*, vol. 29, no. 1, pp. 1311–1318, 2002.

[50] S. Y. Mohamed, L. Cai, F. Khaled et al., "Modeling ignition of a heptane isomer: improved thermodynamics, reaction pathways, kinetics, and rate rule optimizations for 2-methylhexane," *The Journal of Physical Chemistry A*, vol. 120, no. 14, pp. 2201–2217, 2016.

[51] H. J. Curran, P. Gaffuri, W. J. Pitz, C. K. Westbrook, and W. R. Leppard, "Autoignition chemistry of the hexane isomers: An experimental and kinetic modeling study," *SAE Technical Papers*, 1995.

[52] M. Ribaucour, R. Minetti, L. R. Sochet, H. J. Curran, W. J. Pitz, and C. K. Westbrook, "Ignition of isomers of pentane: An experimental and kinetic modeling study," *Proceedings of the Combustion Institute*, vol. 28, no. 2, pp. 1671–1678, 2000.

[53] D. Kang, S. V. Bohac, A. L. Boehman, S. Cheng, Y. Yang, and M. J. Brear, "Autoignition studies of C5 isomers in a motored

engine," *Proceedings of the Combustion Institute*, vol. 36, no. 3, pp. 3597–3604, 2017.

[54] C. K. Westbrook, W. J. Pitz, M. Mehl et al., "Experimental and kinetic modeling study of 2-methyl-2-butene: allylic hydrocarbon kinetics," *The Journal of Physical Chemistry A*, vol. 119, no. 28, pp. 7462–7480, 2015.

[55] S. W. Wagnon, C. L. Barraza-Botet, and M. S. Wooldridge, "Effects of bond location on the ignition and reaction pathways of trans-hexene isomers," *The Journal of Physical Chemistry A*, vol. 119, no. 28, pp. 7695–7703, 2015.

[56] M. Mehl, G. Vanhove, W. J. Pitz, and E. Ranzi, "Oxidation and combustion of the n-hexene isomers: A wide range kinetic modeling study," *Combustion and Flame*, vol. 155, no. 4, pp. 756–772, 2008.

[57] J. R. Peterson, "Alkylate is key for cleaner burning gasoline," *National Meeting of the American Chemical Society (ACS)*, Orlando, FL, 41, 25-30, 1996.

[58] W. G. Lovell, "Knocking characteristics of hydrocarbons," *Industrial & Engineering Chemistry*, vol. 40, no. 12, pp. 2388–2438, Dec 1948.

[59] W. R. Leppard, "A comparison of olefin and paraffin autoignition chemistries: a motored-engine study," *SAE Paper 892081*, pp. 879–904, 1989.

[60] R. Minetti, A. Roubaud, E. Therssen, M. Ribaucour, and L. R. Sochet, "The chemistry of pre-ignition of n-pentane and 1-pentene," *Combustion and Flame*, vol. 118, no. 1-2, pp. 213–220, 1999.

[61] F. Yang, F. Deng, P. Zhang, E. Hu, Y. Cheng, and Z. Huang, "Comparative Study on Ignition Characteristics of 1-Hexene and 2-Hexene behind Reflected Shock Waves," *Energy & Fuels*, vol. 30, no. 6, pp. 5130–5137, 2016.

[62] F. Yang, F. Deng, P. Zhang, Z. Tian, C. Tang, and Z. Huang, "Experimental and Kinetic Modeling Study on trans-3-Hexene Ignition behind Reflected Shock Waves," *Energy & Fuels*, vol. 30, no. 1, pp. 706–716, 2016.

[63] M. Yahyaoui, N. Djebaïli-Chaumeix, C.-E. Paillard et al., "Experimental and modeling study of 1-hexene oxidation behind reflected shock waves," *Proceedings of the Combustion Institute*, vol. 30, no. 1, pp. 1137–1144, 2005.

[64] M. Yahyaoui, N. Djebaïli-Chaumeix, P. Dagaut, C.-E. Paillard, and S. Gail, "Kinetics of 1-hexene oxidation in a JSR and a shock tube: Experimental and modeling study," *Combustion and Flame*, vol. 147, no. 1-2, pp. 67–78, 2006.

[65] M. Yahyaoui, N. Djebaïli-Chaumeix, P. Dagaut, C. Paillard, B. Heyberger, and G. Pengloan, "Ignition and oxidation of 1-hexene/toluene mixtures in a shock tube and a jet-stirred reactor: Experimental and kinetic modeling study," *International Journal of Chemical Kinetics*, vol. 39, no. 9, pp. 518–538, 2007.

[66] M. J. Al Rashidi, M. Mehl, W. J. Pitz, S. Mohamed, and S. M. Sarathy, "Cyclopentane combustion chemistry. Part I: Mechanism development and computational kinetics," *Combustion and Flame*, vol. 183, pp. 358–371, 2017.

[67] M. J. Al Rashidi, S. Thion, C. Togbé et al., "Elucidating reactivity regimes in cyclopentane oxidation: Jet stirred reactor experiments, computational chemistry, and kinetic modeling," *Proceedings of the Combustion Institute*, vol. 36, no. 1, pp. 469–477, 2017.

[68] M. J. Al Rashidi, J. C. Mármol, C. Banyon et al., "Cyclopentane combustion. Part II. Ignition delay measurements and mechanism validation," *Combustion and Flame*, vol. 183, pp. 372–385, 2017.

[69] M. Ribaucour, O. Lemaire, and R. Minetti, "Low-temperature oxidation and autoignition of cyclohexene: A modeling study," *Proceedings of the Combustion Institute*, vol. 29, no. 1, pp. 1303–1309, 2002.

[70] O. Lemaire, M. Ribaucour, M. Carlier, and R. Minetti, "The production of benzene in the low-temperature oxidation of cyclohexane, cyclohexene, and cyclohexa-1,3-diene," *Combustion and Flame*, vol. 127, no. 1-2, pp. 1971–1980, 2001.

[71] S. M. Handford-Styring and R. W. Walker, "Arrhenius parameters for the reaction HO2 + cyclohexane between 673 and 773 K, and for H atom transfer in cyclohexylperoxy radicals," *Physical Chemistry Chemical Physics*, vol. 3, no. 11, pp. 2043–2052, 2001.

[72] A. El Bakali, M. Braun-Unkhoff, P. Dagaut, P. Frank, and M. Cathonnet, "Detailed kinetic reaction mechanism for cyclohexane oxidation at pressure up to ten atmospheres," *Proceedings of the Combustion Institute*, vol. 28, no. 2, pp. 1631–1637, 2000.

[73] S. K. Gulati and R. W. Walker, "Addition of cyclohexane to slowly reacting H2-O2 mixtures at 480°C," *Journal of the Chemical Society, Faraday Transactions 2: Molecular and Chemical Physics*, vol. 85, no. 11, pp. 1799–1812, 1989.

[74] D. Voisin, A. Marchal, M. Reuillon, J.-C. Boettner, and M. Cathonnet, "Experimental and Kinetic Modeling Study of Cyclohexane Oxidation in a JSR at High Pressure," *Combustion Science and Technology*, vol. 138, no. 1-6, pp. 137–158, 1998.

[75] S. M. Daley, A. M. Berkowitz, and M. A. Oehlschlaeger, "A shock tube study of cyclopentane and cyclohexane ignition at elevated pressures," *International Journal of Chemical Kinetics*, vol. 40, no. 10, pp. 624–634, 2008.

[76] B. Sirjean, F. Buda, H. Hakka et al., "The autoignition of cyclopentane and cyclohexane in a shock tube," *Proceedings of the Combustion Institute*, vol. 31, no. 1, pp. 277–284, 2007.

[77] G. Dayma, P. A. Glaude, R. Fournet, and F. Battin-Leclerc, "Experimental and modeling study of the oxidation of cyclohexene," *International Journal of Chemical Kinetics*, vol. 35, no. 7, pp. 273–285, 2003.

[78] S. Vranckx, C. Lee, H. K. Chakravarty, and R. X. Fernandes, "A rapid compression machine study of the low temperature combustion of cyclohexane at elevated pressures," *Proceedings of the Combustion Institute*, vol. 34, no. 1, pp. 377–384, 2013.

[79] Z. Wang, L. Zhao, Y. Wang et al., "Kinetics of ethylcyclohexane pyrolysis and oxidation: An experimental and detailed kinetic modeling study," *Combustion and Flame*, vol. 162, no. 7, pp. 2873–2892, 2015.

[80] F. Billaud, P. Chaverot, M. Berthelin, and E. Freund, "Thermal decomposition of cyclohexane at approximately 810°C," *Industrial & Engineering Chemistry Research*, vol. 27, no. 5, pp. 759–764, 1988.

[81] S. Klaï and F. Baronnet, "Étude de l'oxydation homogène du cyclohexane en phase gazeuse. II. Mécanisme réactionnel et modélisation," *Journal de Chimie Physique et de Physico-Chimie Biologique*, vol. 90, pp. 1951–1998, 1993.

[82] T. J. Snee and J. F. Griffiths, "Criteria for spontaneous ignition in exothermic, autocatalytic reactions: Chain branching and self-heating in the oxidation of cyclohexane in closed vessels," *Combustion and Flame*, vol. 75, no. 3-4, pp. 381–395, 1989.

[83] B. H. Bonner and C. F. H. Tipper, "The cool flame combustion of hydrocarbons I-Cyclohexane," *Combustion and Flame*, vol. 9, no. 3, pp. 317–327, 1965.

[84] A. P. Zeelenberg and H. W. de Bruijn, "Kinetics, mechanism and products of the gaseous oxidation of cyclohexane," *Combustion and Flame*, vol. 9, no. 3, pp. 281–295, 1965.

[85] J. P. Orme, H. J. Curran, and J. M. Simmie, "Shock tube study of 5 membered cyclic hydrocarbon oxidation," in *Proceedings of the European Combustion Meeting*, Louvain-la-Neuve, Belgium, 2005.

[86] V. Simon, Y. Simon, G. Scacchi, and F. Baronnet, "Étude expérimentale et modélisation des réactions d'oxydation du n-pentane et du cyclopentane," *Canadian Journal of Chemistry*, vol. 75, no. 5, pp. 575–584, 1997.

[87] W. J. Pitz, N. P. Cernansky, F. L. Dryer et al., "Development of an experimental database and chemical kinetic models for surrogate gasoline fuels," *SAE Paper 2007-01-0175*, 2007.

[88] Z. Tian, W. J. Pitz, R. Fournet, P.-A. Glaude, and F. Battin-Leclerc, "A detailed kinetic modeling study of toluene oxidation in a premixed laminar flame," *Proceedings of the Combustion Institute*, vol. 33, no. 1, pp. 233–241, 2011.

[89] V. Detilleux and J. Vandooren, "Experimental and kinetic modeling investigation of toluene combustion in premixed, one-dimensional and laminar toluene-oxygen-argon flames," *Proceedings of the Combustion Institute*, vol. 33, no. 1, pp. 217–224, 2011.

[90] Y. Sakai, A. Miyoshi, M. Koshi, and W. J. Pitz, "A kinetic modeling study on the oxidation of primary reference fuel-toluene mixtures including cross reactions between aromatics and aliphatics," *Proceedings of the Combustion Institute*, vol. 32, pp. 411–418, 2009.

[91] Y. Zhang, K. P. Somers, M. Mehl, W. J. Pitz, R. F. Cracknell, and H. J. Curran, "Probing the antagonistic effect of toluene as a component in surrogate fuel models at low temperatures and high pressures. A case study of toluene/dimethyl ether mixtures," *Proceedings of the Combustion Institute*, vol. 36, no. 1, pp. 413–421, 2017.

[92] Y.-D. Liu, M. Jia, M.-Z. Xie, and B. Pang, "Development of a new skeletal chemical kinetic model of toluene reference fuel with application to gasoline surrogate fuels for computational fluid dynamics engine simulation," *Energy & Fuels*, vol. 27, no. 8, pp. 4899–4909, 2013.

[93] D. F. Davidson, B. M. Gauthier, and R. K. Hanson, "Shock tube ignition measurements of iso-octane/air and toluene/air at high pressures," *Proceedings of the Combustion Institute*, vol. 30, no. 1, pp. 1175–1182, 2005.

[94] H.-P. S. Shen and M. A. Oehlschlaeger, "The autoignition of C8H10 aromatics at moderate temperatures and elevated pressures," *Combustion and Flame*, vol. 156, no. 5, pp. 1053–1062, 2009.

[95] S. Honnet, K. Seshadri, U. Niemann, and N. Peters, "A surrogate fuel for kerosene," *Proceedings of the Combustion Institute*, vol. 32, pp. 485–492, 2009.

[96] J.-J. Weng, Y.-X. Liu, B.-Y. Wang, L.-L. Xing, L.-D. Zhang, and Z.-Y. Tian, "Experimental and kinetic investigation of 1,2,4-trimethylbenzene oxidation at low temperature," *Proceedings of the Combustion Institute*, vol. 36, no. 1, pp. 909–917, 2017.

[97] G. Bikas, *Kinetic Mechanism for Hydrocarbon Ignition [PhD Thesis]*, RWTH Aachen, Germany, 2001.

[98] U. Pfahl, K. Fieweger, and G. Adomeit, "Self-ignition of diesel-relevant hydrocarbon-air mixtures under engine conditions," in *Proceedings of the Symposium (International) on Combustion*, vol. 26, pp. 781–789, Elsevier, 1996.

[99] P. Dagaut, M. Reuillon, M. Cathonnet, and D. Voisin, "High pressure oxidation of normal decane and kerosene in dilute conditions from low to high temperature," *Chemistry Physics*, vol. 92, pp. 47–76, 1995.

[100] C. Douté, J. L. Delfau, R. Akrich, and C. Vovelle, "Chemical structure of atmospheric pressure premixed n-decane and kerosene flames," *Combustion Science and Technology*, vol. 106, no. 4-6, pp. 327–344, 1995.

[101] C. Douté, J.-L. Delfau, and C. Vovelle, "Modeling of the structure of a premixed n-decane flame," *Combustion Science and Technology*, vol. 130, no. 1-6, pp. 269–313, 1997.

[102] X. Hui, A. K. Das, K. Kumar, C.-J. Sung, S. Dooley, and F. L. Dryer, "Laminar flame speeds and extinction stretch rates of selected aromatic hydrocarbons," *Fuel*, vol. 97, pp. 695–702, 2012.

[103] D. Bradley, S. E.-D. Habik, and S. A. El-Sherif, "A generalization of laminar burning velocities and volumetric heat release rates," *Combustion and Flame*, vol. 87, no. 3-4, pp. 336–345, 1991.

[104] S. Gaïl and P. Dagaut, "Oxidation of m-xylene in a jsr: Experimental study and detailed chemical kinetic modeling," *Combustion Science and Technology*, vol. 179, no. 5, pp. 813–844, 2007.

[105] S. Saxena, G. Flora, M. Kahandawala, and S. Sidhu, "A shock tube experimental study and kinetic modeling of m-xylene ignition delay," in *Proceedings of the 49th AIAA Aerospace Sciences Meeting including the New Horizons Forum and Aerospace Exposition*, p. 314, Orlando, Fla, USA, 2011.

[106] S. Gudiyella, T. Malewicki, A. Comandini, and K. Brezinsky, "High pressure study of m-xylene oxidation," *Combustion and Flame*, vol. 158, no. 4, pp. 687–704, 2011.

[107] J. L. Emdee, K. Brezinsky, and I. Glassman, "High-temperature oxidation mechanisms of m- and p-xylene," *The Journal of Physical Chemistry*, vol. 95, no. 4, pp. 1626–1635, 1991.

[108] R. J. Johnston and J. T. Farrell, "Laminar burning velocities and Markstein lengths of aromatics at elevated temperature and pressure," *Proceedings of the Combustion Institute*, vol. 30, no. 1, pp. 217–224, 2005.

[109] K. Narayanaswamy, G. Blanquart, and H. Pitsch, "A consistent chemical mechanism for oxidation of substituted aromatic species," *Combustion and Flame*, vol. 157, no. 10, pp. 1879–1898, 2010.

[110] N. M. Marinov, "A detailed chemical kinetic model for high temperature ethanol oxidation," *International Journal of Chemical Kinetics*, vol. 31, no. 2-3, pp. 183–220, 1999.

[111] K. Natarajan and K. A. Bhaskaran, "An Experimental and Analytical Investigation of High Temperature Ignition of Ethanol," in *Proceedings of the 13th International Shock Tube Symposium*, p. 834, Niagara Falls, 1981.

[112] M. P. Dunphy and J. M. Simmie, "High-temperature oxidation of ethanol. Part 1. Ignition delays in shock waves," *Journal of the Chemical Society, Faraday Transactions*, vol. 87, no. 11, pp. 1691–1696, 1991.

[113] F. N. Egolfopoulos, D. X. Du, and C. K. Law, "A study on ethanol oxidation kinetics in laminar premixed flames, flow reactors, and shock tubes," in *Proceedings of the Symposium (international) on combustion*, vol. 24, pp. 833–841, Elsevier, 1992.

[114] P. Dagaut, J. Boettner, and M. Cathonnet, "Kinetic modeling of ethanol pyrolysis and combustion," *Journal de Chimie Physique et de Physico-Chimie Biologique*, vol. 89, pp. 867–884, 1992.

[115] L. R. Cancino, M. Fikri, and A. M. M. Oliveira, "Thermal oxidation of ethanol: experimental and numerical analysis of ignition chemistry of ethanol-air mixtures in shock-heated gases," in *Proceedings of the 27th International Symposium on Shock Waves*, Petersburg, Russia, 2009.

[116] K. A. Heufer and H. Olivier, "Determination of ignition delay times of different hydrocarbons in a new high pressure shock tube," *Shock Waves*, vol. 20, no. 4, pp. 307–316, 2010.

[117] K. A. Heufer, Y. Uygun, and H. Olivier, "Experimental study of the high-pressure ignition of alcohol based biofuels," in *Proceedings of the European Combust Meeting*, 2011.

[118] C. Lee, S. Vranckx, K. A. Heufer et al., "On the chemical kinetics of ethanol oxidation: shock tube, rapid compression machine and detailed modeling study," *Journal of Research in Physical Chemistry*, vol. 226, no. 1, pp. 1–28, 2012.

[119] G. Mittal, S. M. Burke, V. A. Davies, B. Parajuli, W. K. Metcalfe, and H. J. Curran, "Autoignition of ethanol in a rapid compression machine," *Combustion and Flame*, vol. 161, no. 5, pp. 1164–1171, 2014.

[120] C. L. Barraza-Botet, S. W. Wagnon, and M. S. Wooldridge, "Combustion chemistry of ethanol: Ignition and speciation studies in a rapid compression facility," *The Journal of Physical Chemistry A*, vol. 120, no. 38, pp. 7408–7418, 2016.

[121] A. Zyada and O. Samimi Abianeh, "Ethanol kinetic model development and validation at wide range of mixture temperature, pressure and equivalence ratio, under-review," *Fuel*, 2018.

[122] P. S. Veloo, Y. L. Wang, F. N. Egolfopoulos, and C. K. Westbrook, "A comparative experimental and computational study of methanol, ethanol, and n-butanol flames," *Combustion and Flame*, vol. 157, no. 10, pp. 1989–2004, 2010.

[123] T. S. Norton and F. L. Dryer, "An experimental and modeling study of ethanol oxidation kinetics in an atmospheric pressure flow reactor," *International Journal of Chemical Kinetics*, vol. 24, no. 4, pp. 319–344, 1992.

[124] A. Frassoldati, A. Cuoci, T. Faravelli, and E. Ranzi, "Kinetic modeling of the oxidation of ethanol and gasoline surrogate mixtures," *Combustion Science and Technology*, vol. 182, no. 7, pp. 653–667, 2010.

[125] P. Saxena and F. A. Williams, "Numerical and experimental studies of ethanol flames," *Proceedings of the Combustion Institute*, vol. 31, pp. 1149–1156, 2007.

[126] J. Li, A. Kazakov, M. Chaos et al., "Chemical kinetics of ethanol oxidation," in *Proceedings of the 5th US Combustion Meeting*, pp. 25–28, Mar 25, 2007.

[127] W. K. Metcalfe, S. M. Burke, S. S. Ahmed, and H. J. Curran, "A hierarchical and comparative kinetic modeling study of C1 - C2 hydrocarbon and oxygenated fuels," *International Journal of Chemical Kinetics*, vol. 45, no. 10, pp. 638–675, 2013.

[128] C. Olm, T. Varga, É. Valkó, S. Hartl, C. Hasse, and T. Turányi, "Development of an ethanol combustion mechanism based on a hierarchical optimization approach," in *Proceedings of the 7th European Combustion Meeting*, vol. 48, pp. 423–441, Budapest, Hungary, March 30 - April 2, 2015.

[129] P. Dagaut and C. Togbé, "Experimental and modeling study of the kinetics of oxidation of ethanol-gasoline surrogate mixtures (E85 surrogate) in a jet-stirred reactor," *Energy & Fuels*, vol. 22, no. 5, pp. 3499–3505, 2008.

[130] L. R. Cancino, M. Fikri, A. A. M. Oliveira, and C. Schulz, "Ignition delay times of ethanol-containing multi-component gasoline surrogates: Shock-tube experiments and detailed modeling," *Fuel*, vol. 90, no. 3, pp. 1238–1244, 2011.

[131] A. A. Konnov, "Implementation of the NCN pathway of prompt-NO formation in the detailed reaction mechanism," *Combustion and Flame*, vol. 156, no. 11, pp. 2093–2105, 2009.

[132] J. Li, M. Chaos, and A. Kazakov, *Personal communication: Ethanol Model v1. 0*, Princeton University, New Jersey, NJ, USA, 2009.

[133] S. M. Burke, W. Metcalfe, O. Herbinet et al., "An experimental and modeling study of propene oxidation. Part 1: Speciation measurements in jet-stirred and flow reactors," *Combustion and Flame*, vol. 161, no. 11, pp. 2765–2784, 2014.

[134] S. M. Burke, U. Burke, R. Mc Donagh et al., "An experimental and modeling study of propene oxidation. Part 2: Ignition delay time and flame speed measurements," *Combustion and Flame*, vol. 162, no. 2, pp. 296–314, 2015.

[135] S. Ito, "Analysis of aromatic hydrocarbons in gasoline and naphtha with the Agilent 6820 series gas chromatograph and a single polar capillary column," *Agilent Technologies*, 2003.

[136] P. Ghosh, K. J. Hickey, and S. B. Jaffe, "Development of a detailed gasoline composition-based octane model," *Industrial & Engineering Chemistry Research*, vol. 45, no. 1, pp. 337–345, 2006.

[137] DIADEM, *DIPPR Information and Data Evaluation Manager, version 3.1.0*, Brigham Young University, Provo, UT, USA, 2008.

[138] B. E. Pooling, J. M. Prausnitz, and J. P. OConnell, *The Progress of Gasses and Liquids*, McGraw-Hill, New York, NY, USA, 5th edition, 2000.

[139] CHEMKIN-PRO, *Reaction Design Inc*, San Diego, CA, USA, 2010.

[140] Workbench, *Reaction Design Inc*, San Diego, CA, USA, 2010.

[141] D. B. Lenhert, D. L. Miller, N. P. Cernansky, and K. G. Owens, "The oxidation of a gasoline surrogate in the negative temperature coefficient region," *Combustion and Flame*, vol. 156, no. 3, pp. 549–564, 2009.

[142] LLNL Combustion Chemistry, https://www-pls.llnl.gov/?url=science_and_technology-chemistry-combustion.